



1 **Stable carbon isotope deviations in benthic foraminifera as proxy**
2 **for organic carbon fluxes in the Mediterranean Sea**

3

4

5

6 Marc Theodor^{a,*}, Gerhard Schmiedl^a, Frans Jorissen^b, and Andreas Mackensen^c

7

8 ^a Center for Earth System Research and Sustainability, Institute of Geology, University of

9 Hamburg, Bundesstrasse 55, D-20146 Hamburg, Germany

10 ^b CNRS, UMR 6112, LPG–BIAF, Recent and Fossil Bio-Indicators, Université d’Angers, 2

11 Boulevard Lavoisier, 49045 Angers Cedex, France

12 ^c Alfred Wegener Institute Helmholtz Centre for Polar and Marine Research, Am Alten Hafen

13 26, D-27568 Bremerhaven, Germany

14 * Corresponding author

15

16 E-mail addresses: marc.theodor@uni-hamburg.de (M. Theodor), gerhard.schmiedl@uni-

17 hamburg.de (G. Schmiedl), frans.jorissen@univ-angers.fr (F. Jorissen),

18 andreas.mackensen@awi.de (A. Mackensen)



19 Abstract

20 We have determined stable carbon isotope ratios of epifaunal and shallow infaunal benthic
21 foraminifera to relate the inferred gradient of pore water $\delta^{13}\text{C}_{\text{DIC}}$ to varying trophic conditions,
22 and to test the potential of developing a transfer function for organic matter flux rates. The data
23 set is based on samples retrieved from a well-defined bathymetric range (400–1500m water
24 depth) of sub-basins in the western, central and eastern Mediterranean Sea. Regional
25 contrasts in organic matter fluxes and associated $\delta^{13}\text{C}_{\text{DIC}}$ of pore water are recorded by the
26 $\delta^{13}\text{C}$ difference ($\Delta\delta^{13}\text{C}_{\text{Umed-Epi}}$) between the shallow infaunal *Uvigerina mediterranea* and
27 epifaunal species (*Planulina ariminensis*, *Cibicidoides pachydermus*, *Cibicides lobatulus*). The
28 $\Delta\delta^{13}\text{C}_{\text{Umed-Epi}}$ values range from -0.46 to -2.13‰, with generally higher offsets at more eutrophic
29 sites. Because of ontogenetic shifts in the $\delta^{13}\text{C}$ signal of *U. mediterranea* of up to 1.04‰, only
30 tests larger than 600µm were used for the quantitative environmental evaluation. The
31 measured $\delta^{13}\text{C}$ deviations are related to site-specific differences in microhabitat, depth of the
32 principal redox boundary, and TOC content. The $\Delta\delta^{13}\text{C}_{\text{Umed-Epi}}$ values reveal a consistent
33 relation to C_{org} fluxes estimated from satellite-derived surface water primary production in
34 open-marine settings of the Alboran Sea, Mallorca Channel, Strait of Sicily and southern
35 Aegean Sea. In contrast, $\Delta\delta^{13}\text{C}_{\text{Umed-Epi}}$ values in areas affected by intense resuspension and
36 riverine organic matter sources of the northern to central Aegean Sea and the canyon systems
37 of the Gulf of Lions suggest higher C_{org} fluxes compared to the values based on recent surface
38 primary production. Considering the regional biases and uncertainties, a first $\Delta\delta^{13}\text{C}_{\text{Umed-Epi}}$
39 based transfer function for C_{org} fluxes could be established for the Mediterranean Sea.

40

41 Key words: benthic foraminifera, stable carbon isotopes, microhabitat, organic matter fluxes,
42 Mediterranean Sea, transfer function

43



44 1. Introduction

45 The stable isotope composition of benthic foraminifera is used in a wide range of
46 paleoceanographic applications. The $\delta^{18}\text{O}$ signal of benthic foraminifera provides information
47 on bottom water temperature and salinity, and has been applied for the estimation of global
48 ice volume changes (e.g. Shackleton & Opdyke, 1973; Adkins et al., 2002; Marchitto et al.,
49 2014). The benthic foraminiferal $\delta^{13}\text{C}$ signal is mainly used for the reconstruction of changes
50 in deep-sea circulation, bottom water oxygen, and organic carbon fluxes to the sea floor (Curry
51 & Lohmann, 1982; Zahn et al., 1986; McCorkle & Emerson, 1988; Mackensen & Bickert, 1999;
52 Pahnke & Zahn, 2005). Recently, more quantitative approaches have been applied to the
53 reconstruction of past changes in deep-water oxygenation (Stott et al., 2000; Schmiedl &
54 Mackensen, 2006; Hoogakker et al., 2015). There have been also attempts to use multi-
55 species $\delta^{13}\text{C}$ records for the estimation of past organic carbon fluxes (Zahn et al., 1986;
56 Schilman et al., 2003; Kuhnt et al., 2008), however, all of these studies lack a regional
57 calibration based on living specimens and modern environmental data.

58 The $\delta^{13}\text{C}$ gradient of pore water dissolved inorganic carbon (DIC) in the uppermost
59 surface sediment is directly related to the flux and decomposition rates of organic matter
60 (McCorkle & Emerson, 1988; McCorkle et al., 1990; Holsten et al., 2004). With increasing
61 depth in the sediment more isotopically light organic matter (around -18 to -23‰, e.g.
62 Mackensen, 2008) is remineralized by microbial activity (McCorkle et al., 1985). This process
63 results in $\delta^{13}\text{C}_{\text{DIC}}$ pore water depletions of up to -4‰ relative to the bottom water signal
64 (McCorkle & Emerson, 1988; McCorkle et al., 1990; Holsten et al., 2004). The ^{12}C release to
65 the pore water stops when no more OM is remineralized, which mostly coincides with the total
66 consumption of electron acceptors, of which oxygen and nitrate are the usually most important
67 ones (McCorkle & Emerson, 1988; McCorkle et al., 1990; Koho & Pina-Ochoa, 2012,
68 Hoogakker et al., 2015).

69 The $\delta^{13}\text{C}_{\text{DIC}}$ pore water gradient is reflected in the $\delta^{13}\text{C}$ signal of benthic foraminifera
70 from defined microhabitats on and below the sediment–water interface (Grossman, 1984a; b;
71 McCorkle et al., 1990; 1997; Rathburn et al., 1996; Mackensen & Licari, 2004; Schmiedl et al.,



72 2004; Fontanier et al., 2006). Although benthic foraminifera can migrate through the sediment
73 (Linke & Lutze, 1993; Ohga & Kitazato, 1997) and living individuals may occur across a
74 relatively wide depth interval, the $\delta^{13}\text{C}$ signal of a certain species exhibits relatively little
75 scattering, and all specimens tend to reflect the same calcification depth (Mackensen &
76 Douglas, 1989; McCorkle et al., 1990, 1997; Mackensen et al., 2000; Schmiedl et al., 2004).
77 The study of McCorkle & Emerson (1988) has shown that the difference between $\delta^{13}\text{C}_{\text{DIC}}$ of
78 bottom water and $\delta^{13}\text{C}_{\text{DIC}}$ of pore water at the depth in the sediment where oxygen approaches
79 zero is directly related to the oxygen content of the bottom water mass. Based on this
80 observation, the $\delta^{13}\text{C}$ difference of epifaunal (e.g. *Cibicidoides*) and deep infaunal
81 (*Globobulimina*) taxa was used as proxy for the quantification of past changes in deep-water
82 oxygenation (Schmiedl & Mackensen, 2006; Hoogakker et al., 2015). Under the influence of
83 well-oxygenated bottom waters, enhanced organic matter fluxes and associated
84 decomposition rates result in steepening of $\delta^{13}\text{C}_{\text{DIC}}$ gradients in the uppermost sediment, which
85 is then reflected by the $\delta^{13}\text{C}$ difference between epifaunal and shallow infaunal (e.g., *Uvigerina*)
86 species (Zahn et al. 1986; Mackensen et al., 2000; Brückner & Mackensen, 2008). A simple
87 relation between inferred $\delta^{13}\text{C}$ gradients and organic matter fluxes is impeded by the ability of
88 infaunal species to shift their microhabitat in response to changing trophic conditions (Schmiedl
89 & Mackensen, 2006; Theodor et al., 2016). Interspecific differences in the $\delta^{13}\text{C}$ composition of
90 benthic foraminifera are further influenced by species-specific “vital effects”, which can be as
91 large as 1‰ (Schmiedl et al., 2004; McCorkle et al., 2008; Brückner & Mackensen, 2008) and
92 are a reflection of metabolic processes and test calcification rates (McConnaughey, 1989a; b).
93 Of minor impact but still traceable is the influence of carbonate ion concentration and alkalinity
94 gradients in pore waters (Bemis et al., 1998). Finally, significant ontogenetic $\delta^{13}\text{C}$ trends have
95 been documented for certain taxa, particularly for the genera *Uvigerina* and *Bolivina* (Schmiedl
96 et al. 2004; Schumacher et al., 2010; Theodor et al., 2016).

97 The complexity of factors influencing the stable isotope composition of deep-sea benthic
98 foraminifera demonstrates the necessity of isotopic studies on living foraminifera in relation to
99 their biology and microhabitat. In particular, combined ecological and biogeochemical studies



100 on a statistically relevant number of sites and live specimens from areas with well-defined
101 environmental gradients are required for the establishment of reference data sets and transfer
102 functions that could then be used for a more quantitative assessment of organic matter fluxes.
103 The Mediterranean Sea appears particularly suitable for such a study because the present
104 deep-sea environments are characterized by systematically high oxygen contents contrasting
105 with substantial trophic differences. In all basins, sub-surface water masses are highly
106 oxygenated with O_2 concentrations of $>160\mu\text{molkg}^{-1}$ due to frequent replenishment of
107 intermediate water in the Levantine Sea and deep water in the Gulf of Lions, Adriatic Sea, and
108 Aegean Sea (Wüst, 1961; Lascaratos et al., 1999; Pinardi & Masetti, 2000; Tanhua et al., 2013,
109 Pinardi et al., 2015). The inflow of nutrients with Atlantic surface waters causes an overall west-
110 east gradient in primary production, from values of about $225\text{gCm}^{-2}\text{yr}^{-1}$ in the Alboran Sea to
111 about $40\text{gCm}^{-2}\text{yr}^{-1}$ in the extremely nutrient-depleted oligotrophic Levantine Basin (Bosc et al.,
112 2004; Lopez-Sandoval et al., 2011; Puyo-Pay et al., 2011; Huertas et al., 2012; Tanhua et al.,
113 2013, Gogou et al., 2014). In areas influenced by nutrient input through larger rivers and Black
114 Sea outflow, primary production can be locally enhanced, for example leading to a trend of
115 decreasing primary production values along a N-S transect in the Aegean Sea (Lykousis et al.,
116 2002; Skliris et al., 2010). In addition, resuspension and lateral transport of organic matter can
117 lead to locally enhanced food availability in submarine canyons and isolated basins (Puig &
118 Palanques, 1998; Danovaro et al., 1999; Heussner et al., 2006; Canals et al., 2013).

119 In this study we have compiled a data set on the stable carbon isotope composition of
120 life and dead individuals of three epifaunal species (*Cibicidoides pachydermus*, *Planulina*
121 *ariminensis*, *Cibicides lobatulus*) and one shallow infaunal species (*Uvigerina mediterranea*)
122 from 19 Mediterranean sites. The sites are located in a well-defined depth interval (between
123 400 and 1500m) and represent a wide range of trophic conditions. Corrected for ontogenetic
124 effects, the $\Delta\delta^{13}\text{C}_{U_{\text{med}}-E_{\text{epi}}}$ signal was compared to the microhabitat of *U. mediterranea*, the depth
125 of the main redox boundary, TOC content, and organic carbon flux rates calculated from
126 satellite-derived primary production or (if available) flux measurements from sediment trap
127 studies. Major target of this study is the development and evaluation of a transfer function for



128 organic matter fluxes applicable to the quantification of past trophic changes in the
129 Mediterranean Sea.

130

131 **2. Material and methods**

132 This study is based on a compilation of new and published isotope data of multicorer
133 samples retrieved from various Mediterranean sub-basins covering a water depth range of 424
134 to 1466m (Table 1). The study areas include the Alboran Sea and the Mallorca Channel (R.V.
135 *Meteor* cruise M69/1 in August 2006, Hübscher et al., 2010; data published in Theodor et al.,
136 2016), the Gulf of Lions, Spanish Slope off Barcelona and Strait of Sicily (M40/4 in February
137 1998, Hieke et al., 1999; this study and data published in Schmiedl et al., 2004), and the
138 Aegean Sea (M51/3 in November 2001, Hemleben et al., 2003; this study) (Fig. 1). For each
139 station, the sediment color change from yellowish brown to greenish gray was used as an
140 indicator for the change in redox potential from positive to negative values, which serves as an
141 approximation of oxygen consumption and penetration in the surface sediment (Lyle, 1983;
142 Schmiedl et al., 2000).

143 The upper 10cm of the sediment were commonly sliced into 0.5 to 1 cm intervals, in the
144 Aegean Sea into coarser intervals below 3cm, and all samples were subsequently preserved
145 in Rose Bengal stained alcohol (1.5g Rose Bengal per 1l of 96% ethanol) in order to stain
146 cytoplasm of live or recently living foraminifera (Walton, 1952; Bernhard, 2000). In the
147 laboratory, the sediment samples were wet-sieved over a 63µm sieve and after drying at 40°C,
148 dry-sieved over a 150µm (Aegean Sea samples) or 125µm (remaining samples) mesh,
149 respectively. From the coarse fraction of the different down-core intervals, stained individuals
150 of selected epifaunal and shallow infaunal taxa have been counted and the Median Living
151 Depths (MLD; Theodor et al. 2016) were calculated as reference for the respective
152 microhabitat preferences. Only tests with at least three subsequent brightly red colored
153 chambers were considered as living. The low number of stained individuals of epifaunal taxa



154 impeded analyses, except for Site 540B, where stained tests of *C. pachydermus* were
155 available. Likewise, stained tests of *U. mediterranea* were absent at Sites 586 and 589.

156 For stable isotope measurements, stained tests (and unstained tests if no stained tests
157 were available) of three epifaunal species (*C. pachydermus*, *P. ariminensis*, *C. lobatulus*) and
158 one shallow infaunal species (*U. mediterranea*) were selected and each test was measured
159 with a micrometer of an accuracy of 10µm. The stable carbon and oxygen isotope
160 measurements were performed at the Alfred Wegener Institute, Helmholtz Centre for Polar
161 and Marine Research at Bremerhaven with two Finnigan MAT 253 stable isotope ratio mass
162 spectrometers coupled to automatic carbonate preparation devices (Kiel IV). The mass
163 spectrometers were calibrated via international standard NBS 19 to the PDB scale, with results
164 given in δ-notation versus VPDB. Based on an internal laboratory standard (Solnhofen
165 limestone) measured over a one-year period together with samples, the precision of stable
166 isotope measurements was better than 0.06‰ and 0.08‰ for carbon and oxygen, respectively.
167 The δ¹³C difference between epi- and shallow infaunal taxa was calculated as a proxy for the
168 pore water signal, i.e. the δ¹³C gradient between bottom water and shallow pore water DIC.
169 For *U. mediterranea* this procedure was restricted to measurements from the size fraction >600
170 µm in order to minimize ontogenetic effects (Schmiedl et al., 2004; Theodor et al., 2016).

171 Total organic carbon (TOC) concentration in the surface sediment was measured with
172 a Carlo Erba 1500 CNS Analyzer with a precision of 0.02%. Before measurement, CaCO₃ was
173 removed by adding 1N HCl. The TOC values of Sites 596, 601 and 602 were taken from
174 Möbius et al. (2010a; b). Bottom water oxygen concentrations are based on CTD
175 measurements stored in the MedAtlas data set. Primary productivity values in surface waters
176 of the year previously to sampling at each site are based on satellite data of the GlobColour
177 project, and were calculated with the algorithms of Antoine & Morel (1996) as well as Uitz et
178 al. (2008). If available, these estimates were compared with nearby direct primary productivity
179 and export flux measurements. The export fluxes down to the sea floor were estimated
180 according to the function of Betzer et al. (1984) adapted by Felix (2014).

181



182 3. Results

183 Benthic foraminiferal $\delta^{13}\text{C}$ values cover a range of more than 3‰, with higher average
184 values of epifaunal species than the shallow infaunal *Uvigerina mediterranea* (Table 2). The
185 epifaunal species *Cibicidoides pachydermus*, *Cibicides lobatulus* and *Planulina ariminensis*
186 show average values between 1.90‰ at Site 586 (southern Aegean Sea) and -0.16‰ at Site
187 347 (Mallorca Channel) (Table 2; Fig. 2). The highest average epifaunal $\delta^{13}\text{C}_{\text{Epi}}$ values are in
188 the southern and central Aegean Sea (Sites 586, 595), while further to the north at Site 601
189 (northern Aegean Sea) the average $\delta^{13}\text{C}_{\text{Epi}}$ value of 0.87‰ is among the lowest measured. At
190 Site 540B in the Gulf of Lions, the average $\delta^{13}\text{C}_{\text{Epi}}$ value of 1.01‰ is in good agreement with
191 1.00‰ measured by Schmiedl et al. (2004) at the same site. Size-dependent measurements
192 did not reveal any ontogenetic trend in the $\delta^{13}\text{C}$ signal of the epifaunal taxa (supplementary.
193 table 1).

194 For *U. mediterranea* $\delta^{13}\text{C}_{\text{Umed}}$ values vary between -1.41 and 0.85‰ for stained tests
195 and between -1.52 and 1.77‰ for unstained tests (Supplementary Table 1). The highest
196 average values are recorded for the southern Aegean Sea, with 0.58‰ and 1.11‰ for stained
197 and unstained tests, respectively. The lowest average values are recorded for the northern
198 Aegean Sea, with -0.98‰ and -1.13‰ for stained and unstained tests, respectively. The
199 variability at a single site reach 1.38‰ in stained (Site 537) and 2.21‰ in unstained tests (Site
200 586). The ontogenetic $\delta^{13}\text{C}_{\text{Umed}}$ trends are generally comparable for the western Mediterranean
201 Sea and the Strait of Sicily, with $0.11 \pm 0.03\text{‰}(100\mu\text{m})^{-1}$ for stained and $0.07 \pm 0.03\text{‰}(100\mu\text{m})^{-1}$
202 ¹ for unstained tests, except for Site 396 that shows an anomalous negative trend (Table 3;
203 Fig. 3). In the Aegean Sea, the ontogenetic $\delta^{13}\text{C}_{\text{Umed}}$ trends are approximately 50 % steeper
204 with an increase of $0.16 \pm 0.04\text{‰}(100\mu\text{m})^{-1}$ for stained tests. Unstained tests reveal a higher
205 variability and a less steep slope of $0.10 \pm 0.07\text{‰}(100\mu\text{m})^{-1}$ (Table 3, Fig. 3). In order to avoid
206 bias due to ontogenetic effects, only $\delta^{13}\text{C}$ values of *U. mediterranea* tests larger than 600 μm
207 were used for comparison with $\delta^{13}\text{C}_{\text{Epi}}$ values.

208 The calculated $\Delta\delta^{13}\text{C}_{\text{Umed-Epi}}$ values for stained tests range from -0.64‰ in the Gulf of
209 Lion (slope Site) and -0.74‰ (Site 585) to -1.29‰ in the western Mediterranean Sea (sites 347



210 & 540A), to -1.85‰ in the northern Aegean Sea (Site 602) (Table 2). Due to the wider scattering
211 of the $\delta^{13}\text{C}$ values of unstained tests, $\Delta\delta^{13}\text{C}_{Umed-Epi}$ values range from -0.61‰ (Site 589) to -
212 2.0‰ (Site 602) in the Aegean Sea and from -0.55‰ (Site 540B) to -1.06‰ (Site 339) in the
213 western Mediterranean Sea and the Strait of Sicily (Table 2). The magnitude of $\Delta\delta^{13}\text{C}_{Umed-Epi}$
214 values exhibits a relation with trophic conditions at each site, revealing higher differences at
215 more eutrophic sites. Good accordance with the $\Delta\delta^{13}\text{C}_{Umed-Epi}$ show the main redox boundary
216 depth (Fig. 4a) as well as the Median Living Depth of the shallow infaunal *U. mediterranea*
217 (MLD_{Umed}) (Fig. 4b) and less distinctive also the TOC (Fig. 4c). However, a direct correlation
218 with surface water productivity isn't recognizable, neither for stained nor unstained test values
219 (Fig. 4d, e).

220 The MLD_{Umed} , which is used here to describe its microhabitat, increases at the sites
221 with deeper main redox boundaries. The deepest MLD_{Umed} are 2.13 and 2.25cm in the southern
222 Aegean Sea, while the shallowest depths of 0.27cm and 0.38cm are recorded in the central
223 and northern Aegean Sea, respectively (Table 1). In the Gulf of Lions, the MLD_{Umed} is between
224 0.43 and 0.49cm in the axis of the Lacaze–Duthiers Canyon and around 1.22cm at the open
225 slope (Table 1, Fig. 4a). The depth of the sediment color change, which marks the shift in redox
226 potential and thus oxygen penetration, ranges from 2.25cm in the Gulf of Lions (Site 540A) to
227 as much as 30cm in the central Aegean Sea (Site 596) (Table 1, Fig. 4b). The measured TOC
228 contents of the surface sediment range from 0.41 % (Site 586, southern Aegean Sea) and
229 0.58 % (Site 537, Strait of Sicily) to a maximum of 0.82 % (Site 602, northern Aegean Sea)
230 (Table 1, Fig. 4c).

231 The estimated values for annual Primary Production (PP) range from 106 to
232 $294\text{gCm}^{-2}\text{a}^{-1}$. Application of the different algorithms of Antoine & Morel (1996) and Uitz et al.
233 (2008) resulted in an average offset of $54\text{gCm}^{-2}\text{a}^{-1}$, with PP values consistently higher when
234 applying the algorithm of Antoine & Morel (1996). The highest PP values occur in the Alboran
235 Sea ($274\text{--}294$ versus $192\text{--}207\text{gCm}^{-2}\text{a}^{-1}$ according to Uitz et al., 2008) and the northern Aegean
236 Sea ($196\text{--}237$ resp. $139\text{--}164\text{gCm}^{-2}\text{a}^{-1}$), while the lowest PP values occur in the southern and
237 central Aegean Sea ($151\text{--}161$ resp. $106\text{--}116\text{gCm}^{-2}\text{a}^{-1}$) (Table 1).



238

239 **4. Discussion**240 **4.1. Stable carbon isotope signal of epifaunal foraminifera in relation to**
241 **surrounding water masses**

242 The $\delta^{13}\text{C}$ signal of *Cibicidoides pachydermus*, *Cibicides lobatulus*, and *Planulina*
243 *ariminensis* primarily reflects the $\delta^{13}\text{C}_{\text{DIC}}$ of the ambient bottom water since these species
244 appear to prefer an epifaunal microhabitat (Lutze & Thiel, 1989; Kitazato, 1994; Schmiedl et
245 al., 2000). Comparison with published water $\delta^{13}\text{C}_{\text{DIC}}$ measurements confirms $\delta^{13}\text{C}_{\text{Epi}}$ values
246 close to equilibrium also for the Mediterranean Sea (Pierre, 1999; Schmiedl et al., 2004;
247 Theodor et al., 2016). Further, our new data corroborate previous observations of lacking
248 ontogenetic effects in the $\delta^{13}\text{C}_{\text{Epi}}$ signal of these taxa (Corliss et al., 2002; Franco–Fraguas et
249 al., 2011; Theodor et al., 2016) (Supplementary Table 1).

250 In the Alboran Sea (Sites 339 and 347), we measured inter-specific $\delta^{13}\text{C}_{\text{Epi}}$ differences
251 of up to 1.4‰ in unstained individuals. This variability is a result of implausible low $\delta^{13}\text{C}_{\text{Clob}}$
252 values, probably due to a relocation from shallower depths closer to the coast. Conversely, the
253 $\delta^{13}\text{C}_{\text{Cpachy}}$ signal in the Mallorca Channel represents glacial values and is probably affected by
254 the admixture of reworked fossil tests at the sediment surface, as indicated by $\delta^{18}\text{O}$ values of
255 $>4.0\text{‰}$. For all unstained tests also a shift to higher $\delta^{13}\text{C}_{\text{Epi}}$ values due to potential dissolution
256 effects should be considered (Edgar et al., 2013). In order to minimize these effects, a large
257 number of tests, if possible, were measured for *C. pachydermus* and *P. ariminensis*, showing
258 commonly 0.3–0.5‰ higher $\delta^{13}\text{C}$ values for latter species (Table 2, Fig. 2a). Data of *Cibicides*
259 *lobatulus* have only been used for further evaluation where no tests of other species were
260 available for analysis (Fig. 2a; Theodor et al., 2016).

261 The $\delta^{13}\text{C}$ offset between *C. pachydermus* and *P. ariminensis* isn't constant and seems
262 to increase on sites with deeper main redox boundaries. Suggesting a connection therefore
263 with increasing organic matter availability, the varying offsets can be attributed to slight
264 differences in their microhabitat (Table 2; Fig. 2a). While *P. ariminensis* is a strictly epifaunal



265 species, living attached on surfaces on or above the sediment (Lutze & Thiel, 1989), *C.*
266 *pachydermus* commonly lives at or slightly below the sediment–water interface (Rathburn &
267 Corliss, 1994; Schmiedl et al. 2000; Licari & Mackensen, 2005). A very shallow infaunal
268 microhabitat of *C. pachydermus* is corroborated by slightly lower $\delta^{13}\text{C}$ values relative to bottom
269 water $\delta^{13}\text{C}_{\text{DIC}}$ suggesting pore water influence (Schmiedl et al., 2004; Fontanier et al., 2006).
270 In order to compensate for potential pore water effects in the $\delta^{13}\text{C}$ signal of the epifaunal
271 species, the highest $\delta^{13}\text{C}_{\text{Epi}}$ values, mostly of *P. ariminensis*, should be selected for further
272 comparison with shallow infaunal $\delta^{13}\text{C}_{\text{Umed}}$ signals (Table 1).

273 The recorded $\delta^{13}\text{C}_{\text{Epi}}$ values can be related to different Mediterranean water masses
274 (Fig. 2b). The $\delta^{13}\text{C}_{\text{Epi}}$ values of the Gulf of Lions and the Spanish Slope off Barcelona are as
275 low as 0.8‰ suggesting a strong Levantine Intermediate Water (LIW) influence (Pierre, 1999).
276 The $\delta^{13}\text{C}_{\text{Epi}}$ values of the Alboran Sea, the Mallorca Channel, and the Strait of Sicily commonly
277 vary between 1.1 and 1.2‰ and thus reflect the influence of deeper water masses. For the
278 western sites an influence of the Tyrrhenian Deep Water can be assumed. This water mass
279 originates in the Tyrrhenian Sea from a mixture of Levantine Intermediate Water (LIW) and
280 Western Mediterranean Deep Water (WMDW) (Rhein et al., 1999; Send et al., 1999) and is
281 characterized by a $\delta^{13}\text{C}_{\text{DIC}}$ signature between 1.0 to 1.1‰ (Pierre, 1999). For the Strait of Sicily
282 the eastern position explains the influence of less mixed LIW of Eastern Mediterranean origin
283 with a $\delta^{13}\text{C}_{\text{DIC}}$ signature of 1.15‰ (Pierre, 1999).

284 In the Aegean Sea, the broad range of recorded $\delta^{13}\text{C}_{\text{Epi}}$ values of 0.87 to 1.95‰ reflects
285 the strong small-scale oceanographic differences of this region, including presence of various
286 small isolated basins (Figs. 1, 2b). The comparatively high $\delta^{13}\text{C}_{\text{Epi}}$ values of the shallower sites
287 indicate intensified vertical convection at sites of subsurface-water formation, which recently
288 resumed after the stagnation phase of 1994 to 2000 (Androulidakis et al., 2012), although the
289 main deep-water formation area is restricted to the Cretan Sea (Roether et al., 1996;
290 Lascaratos et al., 1999). At greater depth of isolated basins, reduced replenishment of bottom
291 waters (Zervakis et al., 2003; Velaoras & Lascaratos, 2005) is accompanied by relatively low
292 $\delta^{13}\text{C}_{\text{DIC}}$ and accordingly low $\delta^{13}\text{C}_{\text{Epi}}$ values in these environments.



293

294 **4.2. Biological and environmental effects on the stable carbon isotope signal of**
295 ***Uvigerina mediterranea***

296 The size-dependent changes in the $\delta^{13}\text{C}$ signal of *Uvigerina mediterranea* can be
297 attributed to ontogenetic effects. Small tests are depleted in ^{13}C , while larger tests are closer
298 to $\delta^{13}\text{C}_{\text{DIC}}$ of the ambient pore water (Fig. 3). Relatively low $\delta^{13}\text{C}_{U_{med}}$ values of small tests
299 suggest stronger metabolic fractionation in younger individuals (Schmiedl et al., 2004,
300 McCorkle et al., 2008; Schumacher et al., 2010, Theodor et al., 2016). A linear ontogenetic
301 increase of $0.11\text{‰}(100\mu\text{m})^{-1}$ was observed at all sites of the western Mediterranean Sea, while
302 a steeper slope of $0.16\text{‰}(100\mu\text{m})^{-1}$ was recorded in the Aegean Sea (Fig. 3). In addition, the
303 $\delta^{13}\text{C}_{U_{med}}$ values of small individuals from the Aegean Sea were in the order of 1 ‰ lower
304 compared to those from the western Mediterranean Sea.

305 Differences in ontogenetic $\delta^{13}\text{C}$ slopes of the related species *U. peregrina* have been
306 attributed to its highly opportunistic response to regional contrasts in organic matter quantity
307 and quality, and seasonality of supply (Theodor et al., 2016). Obviously, similar effects are also
308 operational in ontogenetic $\delta^{13}\text{C}$ trends of *U. mediterranea*. In the Aegean Sea, this species
309 seems to respond to strong seasonal contrasts in organic matter fluxes (Siokou–Frangou et
310 al., 2002) resulting in particularly high metabolic activity and low $\delta^{13}\text{C}_{U_{med}}$ values in young
311 individuals. A steepening of the $\delta^{13}\text{C}_{U_{med}}$ slopes from the North to the South Aegean Sea has
312 probably the same reasons as for *U. peregrina* in the Western Mediterranean Sea. Because
313 of the higher number of measured tests, this shift of the slope angles is more obvious in
314 unstained than stained tests (Fig. 3). However, even with an increased number of investigated
315 sites compared to Theodor et al. (2016), a similar trend in $\delta^{13}\text{C}_{U_{med}}$ is not recognizable for the
316 Western Mediterranean Sea. This might be caused by lower differences in the annual food
317 supply between the sites or the in total higher input of organic matter compared to the Aegean
318 Sea.

319 The $\delta^{13}\text{C}_{U_{med}}$ values of unstained individuals from 5cm sediment depth in the western
320 Mediterranean Sea and Strait of Sicily are on average 0.1 to 0.2‰ lower than those of live



321 specimens in the topmost centimeter. This adds to previous observations of Theodor et al.
322 (2016) suggesting the influence of the Suess effect (Keeling, 1979; Quay et al., 1992) in live
323 individuals while it is absent in sub-recent specimens. The Suess effect displays the reduction
324 of $\delta^{13}\text{C}$ values in the atmosphere and oceans, due to the anthropogenic release of isotopically
325 light CO_2 out of fossil resources, e.g. oil or coal. A similar effect could not be monitored in the
326 Aegean Sea since live and dead individuals were selected from the same sediment depth
327 suggesting only minor age differences (Table 2, Fig.3). The only exception is Site 595 in the
328 central Aegean Sea, where the deviation is even higher (0.5-0.7‰), when compared to the
329 western Mediterranean Sea. Since this signal is restricted to only one site it could be due to
330 relocation of fossil tests by the effects of bioturbation or lateral sediment transport.

331 Under well-oxygenated conditions, the pore water $\delta^{13}\text{C}_{\text{DIC}}$ gradient depends on the
332 organic matter fluxes and associated decomposition rates of organic matter in the surface
333 sediment (McCorkle and Emerson, 1988; McCorkle et al., 1985, 1990, Holsten et al., 2004).
334 Similarly, organic matter fluxes also control the depth of the oxygenated layer (Rutgers van
335 der Loeff, 1990) and thus the microhabitat range of infaunal foraminifera (Corliss, 1985;
336 Jorissen et al, 1995; Koho et al., 2008; Koho & Pina-Ochoa, 2012). In the Mediterranean Sea
337 subsurface waters are well ventilated resulting in bottom water oxygen concentrations above
338 4.1ml^{-1} at all sites of our study (MedAtlas, 1997). The $\delta^{13}\text{C}$ signal of *U. mediterranea* appears
339 particularly suitable to monitor the pore water $\delta^{13}\text{C}_{\text{DIC}}$ signal in the surface-near sediment
340 because it seems to be less influenced by species-specific “vital effects” (McConnaughey,
341 1989a; b) when compared to other shallow infaunal taxa, for example *U. peregrina* (Schmiedl
342 et al., 2004; Theodor et al., 2016).

343 In this study, the deviation of $\delta^{13}\text{C}_{U_{\text{med}}}$ from bottom water $\delta^{13}\text{C}_{\text{DIC}}$ (reflected as higher
344 $\Delta\delta^{13}\text{C}_{U_{\text{med-Epi}}}$ values, Fig. 4) suggests logarithmic relations with the MLD of *U. mediterranea*,
345 the depth of the oxygenated layer and to the TOC content of the surface sediment. At the more
346 oligotrophic to mesotrophic sites of the Mallorca Channel, the Gulf of Lions, the Spanish Slope
347 off Barcelona, and the southern Aegean Sea, relatively low $\Delta\delta^{13}\text{C}_{U_{\text{med-Epi}}}$ values correspond to
348 a relatively thick oxygenated layer and low TOC contents. The rather deep position of the redox



349 boundary, exceeding 10cm at some sites, enables *U. mediterranea* to inhabit a relatively wide
350 microhabitat range. In contrast, at the more mesotrophic to eutrophic sites of the Alboran Sea
351 relatively high $\Delta\delta^{13}\text{C}_{U_{med-Epi}}$ values coincide with relatively thin oxygenated layers and higher
352 TOC contents. Here, the microhabitat range of *U. mediterranea* is compressed because of
353 limited pore water oxygen (Fig. 4).

354 When comparing sites within the central and northern Aegean Sea, the foraminiferal
355 stable isotope signature and the biogeochemical and ecological characteristics lack a
356 consistent relation (Fig. 4). In these areas strongly negative $\Delta\delta^{13}\text{C}_{U_{med-Epi}}$ do not systematically
357 correspond to maximum TOC contents and the shallowest redox boundary (Fig. 4). The
358 reasons for this absence of a clear relation between $\Delta\delta^{13}\text{C}_{U_{med-Epi}}$ and environmental
359 parameters within this area cannot be unraveled with our available data. It may be related to
360 the high variability in oceanographic and biogeochemical conditions of the bottom water in the
361 isolated basins that are characterized by focusing of sedimentary material (Lykousis et al.,
362 2002; Giresse et al., 2003; Poulos, 2009) and/or temporarily intermittent replenishment of
363 deep-waters on seasonal to decadal time scales (Zervakis et al., 2003; Velaoras & Lascaratos,
364 2005; Androulidakis et al., 2012). The first possibility can increase the supply of refractory and
365 isotopically heavy C_{org} , recorded by higher TOC contents, but with minor effects on the $\delta^{13}\text{C}_{DIC}$
366 pore water gradient. Latter possibility may not just reduce the $\delta^{13}\text{C}_{DIC}$ of the bottom water, but
367 also push the pore water gradient towards stronger differences, explaining the more negative
368 $\Delta\delta^{13}\text{C}_{U_{med-Epi}}$ values, compared to the remaining sites with similar conditions (Fig. 4).

369

370 **4.3. Development of a stable carbon isotope based transfer function for organic** 371 **carbon fluxes**

372 Our results suggest a close relationship between the $\delta^{13}\text{C}$ gradient in the surface
373 sediment (expressed as $\Delta\delta^{13}\text{C}_{U_{med-Epi}}$) and the organic matter (OM) fluxes to the sea floor, for
374 open-ocean settings of the western and central Mediterranean Sea and the southern Aegean
375 Sea (Fig. 5). Based on these observations, we tested the potential for the development of a



376 $\delta^{13}\text{C}$ -based transfer function for OM flux rates. In open-ocean settings, the main food source
377 of deep-sea environments is the exported OM from the surface layer, where photosynthetic
378 Primary Production (PP) takes place (e.g. Boyd & Trull, 2007; Bishop, 2009). The majority of
379 produced particulate organic carbon (POC) is recycled within the photic zone. In the open
380 Mediterranean Sea, around 4% of the POC is exported out of the photic zone, which is lower
381 than for other open oceans, caused by a specific nutrient distribution in the Mediterranean Sea
382 (Moutin & Raimbault, 2002; Gogou et al., 2014). So, the remineralization of organic matter is
383 intensified, which leads to reduced fluxes to the sea floor.

384 During transfer from the surface ocean to the deep-sea, the amount of exported OM
385 decreases exponentially reflecting microbial decay (Suess, 1980; de la Roche & Passow,
386 2007; Packard & Gomez, 2013). Various functions have been developed for the estimation of
387 OM fluxes during sinking of particles through the water column integrating numerous
388 observational data (Suess, 1980; Betzer et al., 1984; Martin et al., 1987; Antia, et al., 2001).
389 The different functions reveal a high variability for the active surface layer, while the results for
390 deeper parts of the water column are within a comparable range (Felix, 2014). In our study
391 (Table 1, Fig.5), we applied the function of Betzer et al. (1984) for calculation of the C_{org} fluxes
392 at the different Mediterranean sites using satellite-borne PP data (Antoine & Morel, 1996; Uitz
393 et al., 2008).

394 A comparison with direct PP and export flux measurements of sediment trap studies
395 revealed ambiguous results. The PP values calculated after Antoine and Morel (1996) are in a
396 comparable range to PP measurements in the western Mediterranean (Moutin & Raimbault,
397 2002; Sanchez-Vidal et al., 2004; 2005; Zúñiga et al., 2007, 2008). However, the estimated
398 export fluxes are too high in these areas compared to the direct measurements of the referred
399 studies, probably due to the aforementioned higher remineralization rate in the Mediterranean
400 Sea. However, the discrepancy in export fluxes is partly compensated by the application of the
401 21–30% lower PP values calculated after Uitz et al. (2008). For the Aegean Sea, in contrast,
402 distinctively higher measured PP values have been reported than were estimated (Siokou–
403 Frangou et al., 2002). For the Gulf of Lions measured OM export fluxes exceed the predicted



404 values (Heussner et al., 2006), which can be explained by the additional lateral input of organic
405 carbon channeled within the local canyon systems (Schmiedl et al., 2000). In order to
406 compensate these possible additional C_{org} fluxes in marginal basin areas, the application of
407 the function of Antoine and Morel (1996) appears more useful, taking into account a potential
408 overestimation of C_{org} fluxes in open-ocean areas.

409 For both approaches of PP calculation (Antoine & Morel, 1996; Uitz et al., 2008) the
410 relation between the estimated C_{org} fluxes and the $\Delta\delta^{13}C_{Umed-Epi}$ exhibits a complex pattern and
411 at first instance lacks a simple and statistically significant correlation (Fig. 5). Particularly,
412 strong negative $\Delta\delta^{13}C_{Umed-Epi}$ in the central and northern Aegean Sea suggest high C_{org} fluxes,
413 which however are not reflected in the estimated PP-based values. The eventual
414 underestimation of C_{org} fluxes in these more marginal areas is likely caused by additional lateral
415 OM input and the focusing of organic matter in isolated small basins. In fact, the northern and
416 central Aegean Sea experiences high OM input from terrestrial sources through North Aegean
417 rivers and the Black Sea outflow (Aksu et al., 1999; Tsiaras et al., 2012). In contrast, the
418 measured main redox boundary depth and the TOC contents do not indicate a higher supply
419 in organic matter. However, sediment trap data from the northern Aegean Sea (Lykousis et al.,
420 2002) reveal C_{org} fluxes of $35\text{--}81\text{gCm}^{-2}\text{a}^{-1}$, which are 3 to 10 times higher than estimated values
421 solely based on PP-based vertical fluxes. Although the high measured values can be partly
422 attributed to the short sampling interval of two months in late spring and thus to elevated
423 vertical fluxes during the spring bloom, elevated year-round lateral C_{org} fluxes can be expected,
424 but on a clearly lower dimension. The measured ratio of primary to reworked OM in the
425 sediment at this site is around 60–70% (Lykousis et al., 2002; Poulos, 2009), which leaves the
426 PP the main source of the C_{org} fluxes to the deep-sea. Similar results have been derived for
427 canyon systems of the Gulf of Lions where OM resuspension, shelf to slope cascading and
428 channeling results in significantly higher observed than PP-derived estimated C_{org} fluxes
429 (Heussner et al., 2006; Pusceddu et al., 2010, Pasqual et al., 2010). Even in open slope
430 settings, resuspended OM can significantly contribute to the total C_{org} flux (McCave et al., 2001;
431 Tesi et al., 2010; Stabholz et al., 2013).



432 Despite these biases, it appears useful to develop a C_{org} flux transfer function at least
433 for the more open marine settings of the western and central Mediterranean Sea and the
434 southern Aegean Sea (Fig. 6). Here, vertical sinking of PP-derived OM appears to be the main
435 source for C_{org} fluxes (Pusceddu et al., 2010) explaining the good correlation with the
436 $\Delta\delta^{13}\text{C}_{U_{\text{med-Epi}}}$ values (Fig. 5). Elevated C_{org} fluxes of the upwelling affected Alboran Sea
437 (Hernandez–Almeida et al., 2011) are reflected in rather negative $\Delta\delta^{13}\text{C}_{U_{\text{med-Epi}}}$ values while in
438 the more oligotrophic regions of the Mallorca Channel, the Spanish Slope off Barcelona, the
439 Strait of Sicily, and the southern Aegean Sea the observed $\delta^{13}\text{C}$ differences are lower. So,
440 omitting the data from the northern and central Aegean Sea, and considering sediment trap
441 data from the Gulf of Lions (Heussner et al., 2006) the derived function can be expressed as

$$442 \quad C_{\text{org}} \text{ flux} = -15.99 * \Delta\delta^{13}\text{C}_{U_{\text{med-Epi}}} + 0.34 \quad (1)$$

443 with a coefficient of determination (R^2) of 0.63 and a significance (p) of 0.0021 (Fig. 6). The
444 estimated C_{org} fluxes can be used to recalculate marine PP, but should be handled carefully,
445 due to the highly possible overestimation caused by lateral advection. Especially in more
446 marginal areas this bias can lead to unreliable recalculated PP values. Likewise, the
447 application outside of the Mediterranean Sea should be biased by differing remineralization
448 rates, due to the specific oceanographic conditions, especially the higher temperatures, in this
449 basin. Therefore, further refinement of this function would require interdisciplinary efforts
450 including a larger number of direct C_{org} flux measurements in sediment trap deployments.

451

452 **5. Conclusions**

453 The $\delta^{13}\text{C}$ signal of deep-sea benthic foraminifera from different areas of the western,
454 central and eastern Mediterranean Sea reflects an integration of various environmental and
455 biological signals. The application of epifaunal benthic foraminifera as an unbiased proxy for
456 the $\delta^{13}\text{C}_{\text{DIC}}$ of the surrounding water mass is ambiguous, due to possible allochthonous tests,
457 but also slight species-specific difference in the microhabitat can result in significant $\delta^{13}\text{C}_{\text{Epi}}$



458 shifts. The $\delta^{13}\text{C}$ signal of the strictly epifaunal *Planulina ariminensis* should be preferred, in
459 contrast to the $\delta^{13}\text{C}$ signal of the very shallow infaunal *Cibicidoides pachydermus*, which seems
460 to be influenced by pore water DIC.

461 The $\delta^{13}\text{C}$ signal of epifaunal taxa lacks ontogenetic effects supporting results from
462 previous studies (Dunbar & Wefer, 1984; Corliss et al, 2002; Theodor et al., 2016). Significant
463 ontogenetic effects were recorded in the $\delta^{13}\text{C}$ signal of *Uvigerina mediterranea*. While the
464 ontogenetic increase of $\delta^{13}\text{C}_{Umed.}$ is more or less comparable ($0.11 \pm 0.03\text{‰}(100\mu\text{m})^{-1}$) in the
465 Western Mediterranean and the Strait of Sicily, a stronger increase and even a regional S-N
466 trend is documented for the Aegean Sea ($0.16 \pm 0.04\text{‰}(100\mu\text{m})^{-1}$). In general, the $\delta^{13}\text{C}$ values
467 of *U. mediterranea* from the Aegean Sea are more negative when compared to those from the
468 western and central Mediterranean Sea. This regional contrast cannot be reconciled with
469 different vital and pore water effects but instead seem to be caused by enhanced residence
470 times of bottom waters in the partly isolated small basins within the Aegean Sea. In cases of
471 well-oxygenated conditions the $\delta^{13}\text{C}_{Umed}$ signal, compared to bottom water, is mainly controlled
472 by regional trophic contrasts and related remineralisation rates. The $\Delta\delta^{13}\text{C}_{Umed-Epi}$ are clearly
473 related to the median microhabitat depth, the depth of the redox boundary (indicating the extent
474 of the oxygenated layer), and to a lower extent to the TOC of the surface sediment. Based on
475 satellite derived primary production estimates C_{org} fluxes were calculated and related to the
476 recorded $\Delta\delta^{13}\text{C}_{Umed-Epi}$ values. Comparison with sediment trap data reveals underestimation of
477 C_{org} fluxes for the marginal areas of the central and northern Aegean Sea and the canyon
478 systems of the Gulf of Lions. In these ecosystems additional lateral transport of resuspended
479 and terrestrial OM contributes substantially to C_{org} fluxes. Considering these biases a first
480 estimation for C_{org} fluxes in open-ocean settings of the Mediterranean Sea could be
481 established.

482

483 Acknowledgements

484 We thank the ship crews and scientists of R/V *Meteor* for good collaboration during cruises
485 M40/4, M51/3, and M69/1. Thanks to Valerie Menke for foraminifera test size measurements



486 and Mareike Paul for selection of epifaunal specimens. We thank David Antoine for
487 suggestions on the GlobColour data set and Jürgen Möbius for support during processing of
488 the TOC samples. Lisa Schönborn and Günther Meyer are thanked for technical support during
489 stable isotope measurements. This study was supported by the Deutsche
490 Forschungsgemeinschaft, grants SCHM1180/16 and MA1942/11.

491

492 **Appendix A.** List of benthic foraminiferal taxa used in this study.

493

494 *Cibicides lobatulus* (Walker & Jakob) = *Nautilus lobatulus* Walker & Jacob, 1798, p. 642, pl.
495 14, fig. 36.

496 *Cibicidoides pachydermus* (Rzehak) = *Truncatulina pachyderma* Rzehak, 1886, p. 87, pl. 1,
497 fig. 5.

498 *Planulina ariminensis* d'Orbigny = *Planulina ariminensis* d'Orbigny, 1826, p. 280, pl. 14, figs.
499 1–3.

500 *Uvigerina mediterranea* Hofker = *Uvigerina mediterranea* Hofker, 1932, p. 118–121, fig. 32.

501

502 **References**

503 Adkins, J.F., McIntyre, K., and Schrag, D.P.: The Salinity, Temperature, and $\delta^{18}\text{O}$ of the
504 Glacial Deep Ocean, *Science*, 298, 1769–1773, doi:10.1126/science.1076252, 2002.

505 Aksu, A.E., Abrajano, T., Mudie, P.J. and Yasar, D.: Organic geochemical and palynological
506 evidence for terrigenous origin of the organic matter in Aegean sapropel S1. *Mar. Geol.*,
507 153, 303–318, doi:10.1016/S0025-3227(98)00077-2, 1999.

508 Androulidakis, Y.S., Kourafalou, V.H., Kresenitis, Y.N., and Zervakis, V.: Variability of deep
509 water mass characteristics in the North Aegean Sea: The role of lateral inputs and
510 atmospheric conditions, *Deep-Sea Res. Pt. I*, 67, 55–72, doi:10.1016/j.dsr.2012.05.004,
511 2012.

512 Antia, A.N., Koeve, W., Fischer, G., Blanz, T., Schulz–Bull, D., Scholten, J., Neuer, S.,
513 Kremling, K., Kuss, J., Peinert, R., Hebbeln, D., Bathmann, U., Conte, M., Fehner, U. and



- 514 Zeitzschel, B.: Basin-wide particulate carbon flux in the Atlantic Ocean: regional export
515 patterns and potential for atmospheric CO₂ sequestration, *Global Biogeochem. Cy.*, 15,
516 845-862, doi: 10.1029/2000GB001376, 2001.
- 517 Antoine, D. and Morel, A.: Oceanic primary production: 1. Adaptation of a spectral light-
518 photosynthesis model in view of application to satellite chlorophyll observations, *Global*
519 *Biogeochem. Cy.*, 10, 43-55, doi:10.1029/95GB02831, 1996.
- 520 Bemis, B.E., Spero, H.J., Bijma, J., and Lea, D.W.: Reevaluation of the oxygen isotopic
521 composition of planktonic foraminifera: Experimental results and revised paleotemperature
522 equations. *Paleoceanography*, 13(2), 150-160, doi:10.1029/98PA00070, 1998.
- 523 Bernhard, J.M.: Distinguishing Live from Dead Foraminifera: Methods Review and Proper
524 Applications, *Micropaleontology*, 46, Supplement 1: Advances in the Biology of
525 Foraminifera, 38-46, 2000.
- 526 Betzer, P.R., Showers, W.J., Laws, E.A., Winn, C.D., DiTullio, G.R., and Kroopnick, P.M.:
527 Primary productivity and particle fluxes on a transect of the equator at 153°W in the Pacific
528 Ocean, *Deep-Sea Res.*, 31, 1-11, doi: 10.1016/0198-0149(84)90068-2, 1984.
- 529 Bishop, J.K.B.: Autonomous observations of the ocean biological carbon pump,
530 *Oceanography*, 22, 182-193, doi:10.5670/oceanog.2009.48, 2009.
- 531 Bosc, E., Bricaud, A., and Antoine, D., 2004. Seasonal and interannual variability in algal
532 biomass and primary production in the Mediterranean Sea, as derived from 4 years of
533 SeaWiFS observations. *Global Biogeochemical Cycles* 18, GB1005,
534 doi:10.1029/2003GB002034, 2004
- 535 Boyd, P.W. and Trull, T.W.: Understanding the export of biogenic particles in oceanic waters:
536 Is there consensus?, *Prog. Oceanogr.*, 72, 276-312, doi:10.1016/j.pcean.2006.10.007,
537 2007.
- 538 Brückner, S. and Mackensen, A.: Organic matter rain rates, oxygen availability, and vital effects
539 from benthic foraminiferal $\delta^{13}\text{C}$ in the historic Skagerrak, North Sea, *Mar. Micropaleontol.*,
540 66, 192-207, doi:10.1016/j.marmicro.2007.09.002, 2008.



- 541 Canals, M., Company, J.B., Martín, D., Sánchez–Vidal, A., and Ramírez–Llodrà, E.: Integrated
542 study of Mediterranean deep canyons: Novel results and future challenges, *Prog.*
543 *Oceanogr.* 118, 1-27, doi:10.1016/j.pocean.2013.09.004, 2013.
- 544 Corliss, B.H.: Microhabitats of benthic foraminifera within deep-sea sediments, *Nature*, 314,
545 435-438, doi:10.1038/314435a0, 1985.
- 546 Corliss, B.H., McCorkle, D.C., and Higdon, D.M.: A time series study of the carbon isotopic
547 composition of deep-sea benthic foraminifera, *Paleoceanography*, 17, 1036,
548 doi:10.1029/2001PA000664, 2002.
- 549 Curry, W.B. and Lohmann, G.P.: Carbon Isotopic Changes in Benthic Foraminifera from the
550 Western South Atlantic: Reconstruction of Glacial Abyssal Circulation Patterns, *Quaternary*
551 *Res.*, 18, 218-235, doi:10.1016/0033-5894(82)90071-0, 1982.
- 552 Danovaro, R., Dinet, A., Duineveld, G., and Tselepides, A.: Benthic response to particulate
553 fluxes in different trophic environments: a comparison between the Gulf of Lions–Catalan
554 Sea (western-Mediterranean) and the Cretan Sea (eastern-Mediterranean), *Prog.*
555 *Oceanogr.*, 44, 287-312, doi:10.1016/S0079-6611(99)00030-0, 1999.
- 556 De La Roche, C. and Passow, U., Factors influencing the sinking of POC and the efficiency of
557 the biological carbon pump, *Deep-Sea Res. Pt. II*, 54, 639-658,
558 doi:10.1016/j.dsr2.2007.01.004, 2007.
- 559 Dunbar, R.B., and Wefer, G.: Stable isotope fractionation in benthic foraminifera from the
560 Peruvian continental margin. *Mar. Geol.*, 59, 215-225, doi:10.1016/0025-3227(84)90094-X
561 1984.
- 562 Edgar, K.M., Pälike, H., and Wilson, P.A.: Testing the impact of diagenesis on the $\delta^{18}\text{O}$ and
563 $\delta^{13}\text{C}$ of benthic foraminiferal calcite from a sediment burial depth transect in the equatorial
564 Pacific, *Paleoceanography*, 28, 468-480, doi:10.1002/palo.20045, 2013.
- 565 Felix, M.: A comparison of equations commonly used to calculate organic carbon content and
566 marine palaeoproductivity from sediment data, *Mar. Geol.*, 347, 1-11,
567 doi:10.1016/j.margeo.2013.10.006, 2014.



- 568 Fontanier, C., Mackensen, A., Jorissen, F.J., Anschutz, P., Licari, L., and Griveau, C.: Stable
569 oxygen and carbon isotopes of live benthic foraminifera from the Bay of Biscay: Microhabitat
570 impact and seasonal variability, *Mar. Micropaleontol.*, 58, 159-183,
571 doi:10.1016/j.marmicro.2005.09.004, 2006.
- 572 Franco-Fraguas, P., Badaraco Costa, K., and de Lima Toledo, F. A.: Stable Isotope/Test size
573 relationship in *Cibicides wuellerstorfi*, *Braz. J. Oceanogr.*, 59, 287-291,
574 doi:10.1590/S1679-87592011000300010, 2011.
- 575 Giresse, P., Buscail, R., and Charrière, B.: Late Holocene multisource material input into the
576 Aegean Sea: depositional and post-depositional processes, *Oceanol. Acta*, 26, 657-672,
577 doi: 10.1016/j.oceact.2003.09.001, 2003.
- 578 Gogou, A., Sanchez-Vidal, A., Durrieu de Madron, X., Stavrakakis, S., Calafat, A.M., Stabholz,
579 M., Psarra, S., Canals, M., Heussner, S., Stavrakaki, I., and Papathanassiou, E.: Carbon
580 flux to the deep in three open sites of the Southern European Seas (SES), *J. Mar. Syst.*,
581 129, 224-233, doi:10.1016/j.jmarsys.2013.05.013, 2014.
- 582 Grossman, E. L.: Carbon isotopic fractionation in live benthic foraminifera – comparison with
583 inorganic precipitate studies, *Geochim. Cosmochim. Acta*, 48, 1505-1512,
584 doi:10.1016/0016-7037(84)90406-X, 1984a.
- 585 Grossman, E. L.: Stable isotope fractionation in live benthic Foraminifera from the Southern
586 California Borderland, *Palaeogeogr. Palaeoclimatol. Palaeoecol.*, 47, 301-327,
587 doi:10.1016/0031-0182(84)90100-7, 1984b.
- 588 Hemleben, C., Becker, T., Bellas, S., Benningsen, G., Casford, J., Cagatay, N., Emeis, K.-C.,
589 Engelen, B., Ertan, T., Fontanier, C., Friedrich, O., Frydas, D., Giunta, S., Hoffelner, H.,
590 Jorissen, F., Kahl, G., Kaszemeik, K., Lykousis, V., Meier, S., Nickel, G., Overman, J.,
591 Pross, J., Reichel, T., Robert, C., Rohling, E., Ruschmeier, W., Sakinc, M., Schiebel, R.,
592 Schmiedl, G., Schubert, K., Schulz, H., Tischnak, J., Truscheit, T.: Ostatlantik – Mittelmeer
593 - Schwarzes Meer, Part 3, Cruise No.51, Leg 3, 14 November – 10 December 2001, Valetta
594 – Istanbul. METEOR-Berichte, Universität Hamburg, 03-1, 57 pp., 2003.



- 595 Hernández–Almeida, I. Bárcena, M.A., Flores, J.A., Sierro, F.J., Sanchez–Vidal, A., Calafat,
596 A.: Microplankton response to environmental conditions in the Alboran Sea (Western
597 Mediterranean): One year sediment trap record. *Mar. Micropaleontol.*, 78, 14-24,
598 doi:10.1016/j.marmicro.2010.09.005, 2011.
- 599 Heussner, S., Durrieu de Madron, X., Calafat, A., Canals, M., Carbonne, J., Delsaut, N., and
600 Saragoni, G.: Spatial and temporal variability of downward particle fluxes on a continental
601 slope: Lessons from an 8-yr experiment in the Gulf of Lions (NW Mediterranean), *Mar.*
602 *Geol.*, 234, 63-92, doi:10.1016/j.margeo.2006.09.003, 2006.
- 603 Hieke, W., Hemleben, C., Linke, P., Türkay, M., Weikert, H.: *Mittelmeer 1998/99, Cruise No.40,*
604 *28 October 1997 – 10 February 1998. METEOR-Berichte, Universität Hamburg, 99-2, 286*
605 *pp., 1999.*
- 606 Holsten, J., Stott, L., and Berelson, W.: Reconstructing benthic carbon oxidation rates using
607 $\delta^{13}\text{C}$ of benthic foraminifera, *Mar. Micropaleontol.*, 53, 117-132, doi:
608 doi:10.1016/j.marmicro.2004.05.006, 2004.
- 609 Hoogakker, B.A.A., Elderfield, H., Schmiedl, G., McCave, I.N., and Rickaby, R.E.M.: Glacial-
610 interglacial changes in bottom-water oxygen content on the Portuguese margin, *Nat.*
611 *Geosci.*, 8, 40-43, doi:10.1038/NGEO2317, 2015.
- 612 Hübscher, C., Betzler, C., Grevemeyer, I.: Sedimentology, rift-processes and neotectonic in
613 the western Mediterranean, Cruise No. 69, 08 August – 20 September 2006, Las Palmas
614 (Spain) – Cartagena (Spain) – La Valletta (Malta). *METEOR-Berichte, Universität Hamburg,*
615 *99-2, 86 pp., 2010.*
- 616 Huertas, I. E., Rios, A. F., Garcia–Lafuente, J., Navarro, G., Makaoui, A., Sanchez–Roman,
617 A., Rodriguez–Galvez, S., Orbi, A., Ruiz, J., and Perez, F. F.: Atlantic forcing of the
618 Mediterranean oligotrophy, *Global Biogeochem. Cycles*, 26, Gb2022,
619 doi:10.1029/2011gb004167, 2012.
- 620 Jorissen, F.J., de Stigter, H.C., and Widmark, J.G.V.: A conceptual model explaining benthic
621 foraminiferal microhabitats, *Mar. Micropaleontol.*, 26, 3-15, doi:10.1016/0377-
622 8398(95)00047-X, 1995.



- 623 Keeling, C.D.: The Suess effect: ¹³Carbon-¹⁴Carbon interrelations, *Environ. Int.*, 2, 229-300,
624 doi:10.1016/0160-4120(79)90005-9, 1979.
- 625 Kitazato, H.: Foraminiferal microhabitats in four marine environments around Japan, *Mar.*
626 *Micropaleontol.*, 24, 29-41, doi:10.1016/0377-8398(94)90009-4, 1994.
- 627 Koho, K.A., García, R., de Stigter, H.C., Epping, E., Koning, E., Kouwenhoven, T.J., and van
628 der Zwaan, G.J.: Sedimentary labile organic carbon and pore water redox control on
629 species distribution of benthic foraminifera: A case study from Lisbon–Setúbal Canyon
630 (southern Portugal), *Prog. Oceanogr.*, 79, 55-82, doi:10.1016/j.pocean.2008.07.004, 2008.
- 631 Koho, K.A. and Piña–Ochoa, E.: Benthic Foraminifera: Inhabitants of low-oxygen
632 environments, in: Altenbach, A.V., Bernhard, J.M., and Seckbach, J. (Eds.): *Anoxia:
633 Evidence for Eukaryote Survival and Paleontological Strategies, Cellular Origin, Life in
634 Extreme Habitats and Astrobiology*, 21, 249–285, doi:10.1007/978-94-007-1896-8_14,
635 2012.
- 636 Kuhnt, T., Schmiedl, G., Ehrmann, W., Hamann, Y., and Andersen, N.: Stable isotope
637 composition of Holocene benthic foraminifers from the Eastern Mediterranean Sea: Past
638 changes in productivity and deep water oxygenation. *Palaeogeogr., Palaeoclimatol.,
639 Palaeoecol.*, 268, 106-115, doi:10.1016/j.palaeo.2008.07.010, 2008.
- 640 Lascaratos, A., Roether, W., Nittis, K., and Klein, B.: Recent changes in the Eastern
641 Mediterranean Deep Waters: a review, *Prog. Oceanogr.*, 44, 5-36, doi:10.1016/S0079-
642 6611(99)00019-1, 1999.
- 643 Licari, L. and Mackensen, A.: Benthic foraminifera off West Africa (1°N to 32°S): Do live
644 assemblages from the topmost sediment reliably record environmental variability?, *Mar.*
645 *Micropaleontol.*, 55, 205-233, doi:10.1016/j.marmicro.2005.03.001, 2005.
- 646 Linke, P. and Lutze, G.F.: Microhabitat preferences of benthic foraminifera a static concept or
647 a dynamic adaptation to optimize food acquisition?, *Mar. Micropaleontol.*, 20, 215-234,
648 doi:10.1016/0377-8398(93)90034-U, 1993.



- 649 López-Sandoval, D. C., Fernández, A., and Marañón, E.: Dissolved and particulate primary
650 production along a longitudinal gradient in the Mediterranean Sea, *Biogeosciences*, 8, 815-
651 825, doi:10.5194/bg-8-815-2011, 2011.
- 652 Lutze, G.F. and Thiel, H.: Epibenthic foraminifera from elevated microhabitats: *Cibicides*
653 *wuellerstorfi* and *Planulina ariminensis*, *J. Foramin. Res.*, 19, 153-158, doi:
654 10.2113/gsjfr.19.2.153, 1989.
- 655 Lykousis, V., Chronis, G., Tselepidis, A., Price, B., Theocharis, A., Siokou-Frangou, I., Van
656 Wambeke, F., Danovaro, R., Stavrakakis, S., Duineveld, G., Georgopoulos, D., Ignatiades,
657 L., Souvermezoglou, E., and Voutsinou-Taliadouri, F.: Major outputs of the recent
658 multidisciplinary biogeochemical researches undertaken in the Aegean Sea, *J. Marine*
659 *Syst.*, 33–34, 313–334, doi:10.1016/S0924-7963(02)00064-7, 2002.
- 660 Lyle, M.: The brown-green color transition in marine sediments: A marker of the Fe(III)-Fe(II)
661 redox boundary. *Limnol. Oceanogr.*, 28, 1026-1033, doi:10.4319/lo.1983.28.5.1026, 1983.
- 662 Mackensen, A.: On the use of benthic foraminiferal $\delta^{13}\text{C}$ in palaeoceanography: constraints
663 from primary proxy relationships, in: Austin, W.E.N. and James, R.H. (eds.):
664 *Biogeochemical Controls on Palaeoceanographic Environmental Proxies*, Geological
665 Society, London, Special Publications 303, pp. 121–133, doi:10.1144/SP303.9, 2008.
- 666 Mackensen, A., and Bickert, T.: Stable carbon isotopes in benthic foraminifera: Proxies for
667 deep and bottom water circulation and new production. In: Fischer, G., and Wefer, G. (Eds.),
668 *Use of proxies in paleoceanography: Examples from the South Atlantic*. Springer, Berlin,
669 Heidelberg, pp. 229-254, doi:10.1007/978-3-642-58646-0_9, 1999.
- 670 Mackensen, A., and Douglas, R.G.: Down-core distribution of live and dead deep-water benthic
671 foraminifera in box cores from the Weddell Sea and the California continental borderland,
672 *Deep-Sea Res.*, 36, 879-900, doi:10.1016/0198-0149(89)90034-4, 1989.
- 673 Mackensen, A., and Licari, L.: Carbon isotopes of live benthic foraminifera from the eastern
674 South Atlantic Ocean: Sensitivity to organic matter rain rates and bottom water carbonate
675 saturation state. In: Wefer, G., Mulitza, S., and Rathmeyer, V. (Eds.), *The South Atlantic in*



- 676 the Late Quaternary - Reconstruction of material budget and current systems. Springer-
677 Verlag, Berlin, pp. 623-644, doi:10.1007/978-3-642-18917-3_27, 2004.
- 678 Mackensen, A., Schumacher, S., Radke, J., and Schmidt, D.N.: Microhabitat preferences and
679 stable carbon isotopes of endobenthic foraminifera: clue to quantitative reconstruction of
680 oceanic new production?, *Mar. Micropaleontol.*, 40, 233-258, doi:10.1016/S0377-
681 8398(00)00040-2, 2000.
- 682 Marchitto, T.M., Curry, W.B., Lynch-Stieglitz, J., Bryan, S.P., Cobb, K.M., and Lund, D.C.:
683 Improved oxygen isotope temperature calibrations for cosmopolitan benthic foraminifera,
684 *Geochimica et Cosmochimica Acta*, 130, 1–11, doi:10.1016/j.gca.2013.12.034, 2014.
- 685 Martin, J.H., Knauer, G.A., Karl, D.M., and Broenkow, W.W.: VERTEX: carbon cycling in the
686 northeast Pacific, *Deep-Sea Res.*, 34, 267-285, doi:10.1016/0198-0149(87)90086-0, 1987.
- 687 McCave, I.N., Hall, I.R., Antia, A.N., Chou, L., Dehairs, F., Lampitt, R.S., Thomsen, L., van
688 Weering, T.C.E., and Wollast, R.: Distribution, composition and flux of particulate material
689 over the European margin at 47°–50°N, *Deep-Sea Res. Pt. II*, 48, 3107–3139,
690 doi:10.1016/S0967-0645(01)00034-0, 2001.
- 691 McConnaughey T.: 13C and 18O isotopic disequilibrium in biological carbonates: I. Patterns,
692 *Geochim. Cosmochim. Acta*, 53, 151-162, doi:10.1016/0016-7037(89)90282-2, 1989a.
- 693 McConnaughey T. 13C and 18O isotopic disequilibrium in biological carbonates: II. in vitro
694 simulation of kinetic isotope effects, *Geochim. Cosmochim. Acta*, 53, 163-171,
695 doi:10.1016/0016-7037(89)90283-4, 1989b.
- 696 McCorkle, D.C. and Emerson, S.R.: The relationship between pore water carbon isotopic
697 composition and bottom water oxygen concentration, *Geochim. Cosmochim. Acta*, 52,
698 1169-1178, doi:10.1016/0016-7037(88)90270-0, 1988.
- 699 McCorkle, D.C., Bernhard, J.M., Hintz, C.J., Blanks, J.K., Chandler, G.T., and Shaw, T.J.: The
700 carbon and oxygen stable isotopic composition of cultured benthic foraminifera, in: Austin,
701 W.E.N. and James, R.H. (eds.): *Biogeochemical Controls on Palaeoceanographic*
702 *Environmental Proxies*, Geological Society, London, Special Publications 303, 135-154,
703 doi:10.1144/SP303.10, 2008.



- 704 McCorkle, D.C., Corliss, B.H., and Farnham, C.A.: Vertical distributions and stable isotopic
705 compositions of live (stained) benthic foraminifera from the North Carolina and California
706 continental margins, *Deep-Sea Res. Pt. I*, 44, 983-1024, doi:10.1016/S0967-
707 0637(97)00004-6, 1997.
- 708 McCorkle, D.C., Emerson, S.R., and Quay, P.D.: Stable carbon isotopes in marine porewaters,
709 *Earth Planet. Sc. Lett.*, 74, 13-26, doi:10.1016/0012-821X(85)90162-1, 1985.
- 710 McCorkle, D.C., Keigwin, L.D., Corliss, B.H., and Emerson, S.R.: The influence of
711 microhabitats on the carbon isotopic composition of deep-sea benthic foraminifera,
712 *Paleoceanography*, 5, 161-185, doi:10.1029/PA005i003p00295, 1990.
- 713 MedAtlas, 1997. Mediterranean Hydrographic Atlas (Mast Supporting Initiative; MAS2-CT93-
714 0074): CD-ROM.
- 715 Möbius, J., Lahajnar, N., and Emeis, K.-C.: Diagenetic control of nitrogen isotope ratios in
716 Holocene sapropels and recent sediments from the Eastern Mediterranean Sea,
717 *Biogeosciences*, 7, 3901-3914, doi:10.5194/bg-7-3901-2010, 2010a.
- 718 Möbius, J Lahajnar, N., and Emeis, K.-C.: Chemical composition of surface sediment samples
719 from the Eastern Mediterranean Sea. doi:10.1594/PANGAEA.754732, 2010b.
- 720 Moutin, T. and Raimbault, P.: Primary production, carbon export and nutrients availability in
721 western and eastern Mediterranean Sea in early summer 1996 (MINOS cruise), *J. Marine*
722 *Syst.*, 33-34, 273-288, doi: 10.1016/S0924-7963(02)00062-3, 2002.
- 723 Ohga, T. and Kitazato, H.: Seasonal changes in bathyal foraminiferal populations in response
724 to the flux of organic matter (Sagami Bay, Japan), *Terra Nova*, 9, 33-37, doi:10.1046/j.1365-
725 3121.1997.d01-6.x, 1997.
- 726 Packard, T.T. and Gómez, M.: Modeling vertical carbon flux from zooplankton respiration,
727 *Prog. Oceanogr.*, 110, 59-68, doi:10.1016/j.pocean.2013.01.003, 2013.
- 728 Pahnke, K., and Zahn, R.: Southern hemisphere water mass conversion with North Atlantic
729 climate variability. *Science*, 307, 1741-1746, doi:10.1126/science.1102163, 2005.
- 730 Pasqual, C., Sanchez-Vidal, A., Zúñiga, D., Calafat, A., Canals, M., Durrieu de Madron, X.,
731 Puig, P., Heussner, S., Palanques, A., and Delsaut, N.: Flux and composition of settling



- 732 particles across the continental margin of the Gulf of Lion: the role of dense shelf water
733 cascading, *Biogeosciences*, 7, 217-231, doi:10.5194/bg-7-217-2010, 2010.
- 734 Pierre, C.: The oxygen and carbon isotope distribution in the Mediterranean water masses,
735 *Mar. Geol.*, 153, 41-55, doi:10.1016/S0025-3227(98)00090-5, 1999.
- 736 Pinardi, N. and Masetti, E.: Variability of the large scale general circulation of the
737 Mediterranean Sea from observations and modelling: a review, *Palaeogeogr.*
738 *Palaeoclimatol. Palaeoecol.*, 158, 153-173, doi:10.1016/S0031-0182(00)00048-1, 2000.
- 739 Pinardi, N., Zavatarelli, M., Adani, M., Coppini, G., Fratianni, C., Oddo, P., Simoncelli, S.,
740 Tonani, M, Lyubartsev, V., Dobricic, S. and Bonaduce, A.: Mediterranean Sea large-scale
741 low-frequency ocean variability and water mass formation rates from 1987 to 2007: A
742 retrospective analysis, *Prog. Oceanogr.* 132, 318-332, doi:10.1016/j.pcean.2013.11.003,
743 2015.
- 744 Poulos, S.E.: Origin and distribution of the terrigenous component of the unconsolidated
745 surface sediment of the Aegean floor: A synthesis, *Cont. Shelf Res.*, 29, 2045–2060,
746 doi:10.1016/j.csr.2008.11.010, 2009.
- 747 Puig, P. and Palanques, A.: Temporal variability and composition of settling particle fluxes on
748 the Barcelona continental margin (Northwestern Mediterranean), *J. Mar. Res.*, 56, 639-654,
749 doi:10.1357/002224098765213612, 1998.
- 750 Pujó-Pay, M., Conan, P., Oriol, L., Cornet–Barthaux, V., Falco, C., Ghiglione, J.-F., Goyet, C.,
751 Moutin, T., and Prieur, L.: Integrated survey of elemental stoichiometry (C,N,P) from the
752 western to eastern Mediterranean Sea, *Biogeosciences*, 8, 883-899, doi:10.5194/bg-8-883-
753 2011, 2011.
- 754 Pusceddu, A., Bianchelli, S., Canals, M., Sanchez–Vidal, A., Durrieu de Madron, X., Heussner,
755 S., Lykousis, V., de Stigter, H., Trincardi, F., and Danovaro, R.: Organic matter in sediments
756 of canyons and open slopes of the Portuguese, Catalan, Southern Adriatic and Cretan Sea
757 margins, *Deep-Sea Res. Pt. I*, 57, 441–457, doi:10.1016/j.dsr.2009.11.008, 2010a.
- 758 Quay, P.D., Tilbrook, B., and Wong, C.S.: Oceanic Uptake of Fossil Fuel CO₂: Carbon-13
759 Evidence, *Science*, 256, 74-79, doi: 10.1126/science.256.5053.74, 1992.



- 760 Rathburn, A.E. and Corliss, B.H.: The ecology of living (stained) deep-sea benthic foraminifera
761 from the Sulu Sea, *Paleoceanography*, 9, 87-150, doi: 10.1029/93PA02327, 1994.
- 762 Rathburn, A.E., Corliss, B.H., Tappa, K.D., and Lohmann, K.C.: Comparisons of the ecology
763 and stable isotopic compositions of living (stained) benthic foraminifera from the Sulu and
764 South China Seas, *Deep-Sea Res. Pt. I*, 43, 1617-1646, doi:10.1016/S0967-
765 0637(96)00071-4, 1996.
- 766 Rhein, M., Send, U., Klein, B., and Krahnemann, G.: Interbasin deep water exchange in the
767 western Mediterranean. *J. Geophys. Res.* 104 (C10), 23,495–23,508,
768 doi:10.1029/1999JC900162, 1999.
- 769 Roether, W., Manca, B. B., Klein, B., Bregant, D., Georgopoulos, D., Beitzel, V., Kovacevic,
770 V., and Luchetta, A.: Recent changes in eastern Mediterranean deep waters, *Science*, 271,
771 333-335, doi: 10.1126/science.271.5247.333, 1996.
- 772 Rutgers van der Loeff, M.M.: Oxygen in pore waters of deep-sea sediments, *Philos. Trans. R.*
773 *Soc. London, Ser. A*, 331, 69-84, doi: 10.1098/rsta.1990.0057, 1990.
- 774 Sanchez–Vidal, A., Calafat, A., Canals, M., and Fabres, J.: Particle fluxes in the Almeria-Oran
775 Front: control by coastal upwelling and sea surface circulation, *J. Mar. Syst.*, 52, 89-106,
776 doi:10.1016/j.jmarsys.2004.01.010, 2004.
- 777 Sanchez–Vidal, A., Calafat, A., Canals, M., Frigola, J., and Fabres, J.: Particle fluxes and
778 organic carbon balance across the Eastern Alboran Sea (SW Mediterranean Sea), *Cont.*
779 *Shelf Res.*, 25, 609-628, doi:10.1016/j.csr.2004.11.004, 2005.
- 780 Send, U., Font, J., Krahnemann, G., Millot, C., Rhein, M., and Tintore, J.: Recent advances in
781 observing the physical oceanography of the western Mediterranean Sea. *Prog. Oceanogr.*
782 44, 37–64, doi:10.1016/S0079-6611(99)00020-8, 1999.
- 783 Schilman, B., Almogi–Labin, A., Bar–Matthews, M., and Luz, B.: Late Holocene productivity
784 and hydrographic variability in the eastern Mediterranean inferred from benthic foraminiferal
785 stable isotopes. *Paleoceanography*, 18, doi:10.1029/2002PA000813, 2003.



- 786 Schmiedl, G. and Mackensen, A.: Multispecies stable isotopes of benthic foraminifers reveal
787 past changes of organic matter decomposition and deepwater oxygenation in the Arabian
788 Sea, *Paleoceanography*, 21, PA4213, doi:10.1029/2006PA001284, 2006.
- 789 Schmiedl, G., de Bovée, F., Buscail, R., Charrière, B., Hemleben, C., Medernach, L., and
790 Picon, P.: Trophic control of benthic foraminiferal abundance and microhabitat in the bathyal
791 Gulf of Lions, western Mediterranean Sea, *Mar. Micropaleontol.*, 40, 167-188,
792 doi:10.1016/S0377-8398(00)00038-4, 2000.
- 793 Schmiedl, G., Pfeilsticker, M., Hemleben, C., and Mackensen, A.: Environmental and biological
794 effects on the stable isotope composition of recent deep-sea benthic foraminifera from the
795 western Mediterranean Sea, *Mar. Micropaleontol.*, 51, 129-152,
796 doi:10.1016/j.marmicro.2003.10.001, 2004.
- 797 Schumacher, S., Jorissen, F.J., Mackensen, A., Gooday, A.J., and Pays, O.: Ontogenetic
798 effects on stable carbon and oxygen isotopes in tests of live (Rose Bengal stained) benthic
799 foraminifera from the Pakistan continental margin, *Mar. Micropaleontol.*, 76, 92-103,
800 doi:10.1016/j.marmicro.2010.06.002, 2010.
- 801 Shackleton, N.J. and Opdyke, N.D.: Oxygen Isotope and Palaeomagnetic Stratigraphy of
802 Equatorial Pacific Core V28-238: Oxygen Isotope Temperatures and Ice Volumes on a 105
803 Year and 106 Year Scale, *Quat. Res.*, 3, 39-55, doi:10.1016/0033-5894(73)90052-5, 1973.
- 804 Siokou-Frangou, I., Bianchi, M., Christaki, U., Christou, E. D., Giannakourou, A., Gotsis, O.,
805 Ignatiades, L., Pagou, K., Pitta, P., Psarra, S., Souvermezoglou, E., Van Wambeke, F., and
806 Zervakis, V.: Carbon flow in the planktonic food web along a gradient of oligotrophy in the
807 Aegean Sea (Mediterranean Sea), *J. Mar. Syst.*, 33-34, 335-353, doi:10.1016/S0924-
808 7963(02)00065-9, 2002.
- 809 Skliris, N., Mantziafou, A., Sofianos, S., and Gkanaos, A.: Satellite-derived variability of the
810 Aegean Sea ecohydrodynamics, *Cont. Shelf Res.* 30, 403-418,
811 doi:10.1016/j.csr.2009.12.012, 2010.
- 812 Stabholz, M., Durrieu de Madron, X., Canals, M., Khripounoff, A., Taupier-Letage, I., Testor,
813 P., Heussner, S., Kerhervé, P., Delsaut, N., Houpert, L., Lastras, G., and Dennielou, B.:



- 814 Impact of open-ocean convection on particle fluxes and sediment dynamics in the deep
815 margin of the Gulf of Lions, *Biogeosciences*, 10, 1097-1116, doi:10.5194/bg-10-1097-2013,
816 2013.
- 817 Stott, L.D., Berelson, W., Douglas, R., and Gorsline, D., 2000. Increased dissolved oxygen in
818 Pacific intermediate waters due to lower rates of carbon oxidation in sediments. *Nature*,
819 407, 367-370, doi:10.1038/35030084, 2000.
- 820 Suess, E.: Particulate organic carbon flux in the oceans - surface productivity and oxygen
821 utilization, *Nature*, 288, 260–263, doi:10.1038/288260a0, 1980.
- 822 Tanhua, T., Hainbucher, D., Schroeder, K., Cardin, V., Álvarez, M., and Civitarese, G.: The
823 Mediterranean Sea system: a review and an introduction to the special issue, *Ocean Sci.*,
824 9, 789-803, doi:10.5194/os-9-789-2013, 2013.
- 825 Tesi, T., Puig, P., Palanques, A., and Goñi, M.A.: Lateral advection of organic matter in
826 cascading-dominated submarine canyons, *Prog. Oceanogr.*, 84, 185-203,
827 doi:10.1016/j.pocean.2009.10.004, 2010.
- 828 Theodor, M., Schmiedl, G., and Mackensen, A.: Stable isotope composition of deep-sea
829 benthic foraminifera under contrasting trophic conditions in the western Mediterranean Sea,
830 *Mar. Micropaleontol.*, 124, 16-28, doi:10.1016/j.marmicro.2016.02.001, 2016.
- 831 Tsiaras, K.P., Kourafalou, V.H., Raitsos, D.E., Triantafyllou, G., Petihakis, G., and Korres, G.:
832 Inter-annual productivity variability in the North Aegean Sea: Influence of thermohaline
833 circulation during the Eastern Mediterranean Transient, *J. Mar. Syst.*, 96-97, 72-81,
834 doi:10.1016/j.jmarsys.2012.02.003, 2012.
- 835 Uitz, J., Huot, Y., Bruyant, F., Babin, M., and Claustre, H.: Relating phytoplankton
836 photophysiological properties to community structure on large scales, *Limnol. Oceanogr.*,
837 53, 614-630, doi:10.4319/lo.2008.53.2.0614, 2008.
- 838 Velaoras, D. and Lascaratos, A.: Deep water mass characteristics and interannual variability
839 in the North and Central Aegean Sea, *J. Mar. Syst.*, 53, 59-85,
840 doi:10.1016/j.jmarsys.2004.05.027, 2005.



- 841 Walton, W.R.: Techniques for recognition of living foraminifera, Contributions from the
842 Cushman Foundation for Foraminiferal Research, 3, 56-60, 1952.
- 843 Wüst, G.: On the vertical circulation of the Mediterranean Sea. J. Geophys. Res. 66, 3261–
844 3271, doi:10.1029/JZ066i010p03261, 1961.
- 845 Zahn, R., Winn, K., and Sarnthein, M.: Benthic Foraminiferal $\delta^{13}\text{C}$ and accumulation rates of
846 organic Carbon: *Uvigerina peregrina* group and *Cibicidoides wuellerstorfi*,
847 Paleocceanography, 1, 27-42, doi:10.1029/PA001i001p00027, 1986.
- 848 Zervakis, V., Krasakopoulou, E., Georgopoulos, D., and Souvermezoglou, E.: Vertical diffusion
849 and oxygen consumption during stagnation periods in the deep North Aegean, Deep-Sea
850 Res. Pt. I, 50, 53-71, doi:10.1016/S0967-0637(02)00144-9, 2003.
- 851 Zúñiga, D., Calafat, A., Sanchez–Vidal, A., Canals, M., Price, B., Heussner, S., and Miserocchi,
852 S.: Particulate organic carbon budget in the open Algero-Balearic Basin (Western
853 Mediterranean): Assessment from a one-year sediment trap experiment, Deep-Sea Res.
854 Pt. I, 54, 1530-1548, doi:10.1016/j.dsr.2007.06.001, 2007.
- 855 Zúñiga, D., Calafat, A., Heussner, S., Miserocchi, S., Sanchez–Vidal, A., Garcia–Orellana, J.,
856 Canals, M., Sánchez–Cabeza, J.A., Carbonne, J., Delsaut, N., Saragoni, G.: Compositional
857 and temporal evolution of particle fluxes in the open Algero–Balearic basin (Western
858 Mediterranean), J. Mar. Syst., 70, 196-214, doi:10.1016/j.jmarsys.2007.05.007, 2008.



859 **Table captions**

860 Table 1. Position, water depth, median living depth (MLD) of *Uvigerina mediterranea*,
861 geochemical, Primary Production (PP) and C_{org} flux values of the investigated multicorer sites.
862 Annual PP values are averages for the year previous to sampling after data from the
863 GlobColour project. C_{org} fluxes were calculated after Betzer et al. (1984) and the MLD after
864 Theodor et al. (2016).

865

866 Table 2. Average stable carbon isotope composition of selected benthic foraminifera with
867 standard deviations. Underlined values of epifaunal species were applied to estimated bottom
868 water $\delta^{13}C_{DIC}$. Also given are values for *Uvigerina mediterranea* tests larger than 600 μ m and
869 the difference of this species compared to the average epifaunal stable carbon isotope ratios
870 ($\Delta\delta^{13}C_{Umed-Epi}$).

871

872 Table 3. Linear regressions of ontogenetic trends of $\delta^{13}C_{Umed}$. The measured number of stained
873 and unstained tests as well as the significance values are added.



874 Table 1.

Site	latitude	longitude	station depth (m)	MLD _{mixed} (cm)	redox boundary depth (cm)	TOC (%)	PP (gCm ⁻² a ⁻¹)	C _{org} flux (gCm ⁻² a ⁻¹)
537	37°02.14' N	13°11.35' E	472	0.83	2.75	0.560	173.06	12.26
540A	42°27.69' N	03°25.64' E	911	0.43	2.25		203.97	10.22
540B	42°25.70' N	03°41.34' E	812	1.22	7	0.750	193.99	10.24
540C	41°21.04' N	03°01.36' E	721	0.97	4.25	0.650	179.74	9.91
585	36°39.60' N	25°55.72' E	708	2.25	21	0.430	151.13	7.85
586	36°34.32' N	25°57.91' E	424	1.00	18	0.408	151.13	10.83
589	36°45.19' N	26°35.38' E	584	2.13	14.5	0.698	150.87	8.84
592	37°47.65' N	26°15.72' E	1148	0.38	16	0.630	151.46	5.81
595	38°15.63' N	25°06.17' E	662	0.56	19		159.63	8.84
596	38°57.32' N	24°45.20' E	884	0.41	30	0.730	160.50	7.43
599	39°45.36' N	24°05.61' E	1084	0.47	16.5	0.579	195.88	8.66
601	40°05.22' N	24°36.62' E	977	0.27	6	0.750	206.68	9.97
602	40°13.03' N	24°15.39' E	1466	0.78	4	0.820	236.78	9.36
338	36°15.03' N	03°24.98' W	732	0.55	1.75	0.832	294.00	19.64
339	36°18.30' N	03°08.39' W	849	0.81	2.25	0.766	280.09	16.71
347	36°27.90' N	02°55.50' W	629	0.63	1.5	0.835	273.71	19.53
394	38°53.39' N	02°38.40' E	646	1.28	8		171.05	9.90
395	38°57.70' N	02°31.51' E	834	0.81	7	0.463	170.54	8.40
396	39°09.60' N	02°28.78' E	562	0.88	10	0.403	167.82	10.52
Canyon ø	42°27.60' N	03°29.80' E	920	1.50	4	0.870		19.7
Canyon feb	42°27.60' N	03°29.80' E	920	0.49				
Canyon aug	42°27.60' N	03°29.80' E	920	2.50				
Slope ø	42°25.60' N	03°42.00' E	800	1.81	11	0.720		12.8
Slope feb	42°25.60' N	03°42.00' E	800	3.21				
Slope aug	42°25.60' N	03°42.00' E	800	0.41				

875



876 Table 2.

Site	$\delta^{13}\text{C}_{\text{Pari}}$ (‰ VPDB)	st. dev. (‰)	$\delta^{13}\text{C}_{\text{Qrac}}$ (‰ VPDB)	st. dev. (‰)	$\delta^{13}\text{C}_{\text{Clob}}$ (‰ VPDB)	st. dev. (‰)	$\delta^{13}\text{C}_{\text{Epi}}$ (‰ VPDB)	st. dev. (‰)
537			<u>1.11</u>	<u>0.32</u>			1.11	0.32
540A	<u>1.08</u>	<u>0.14</u>	0.76	0.17			1.08	0.14
540B	<u>0.99</u>		<u>1.01</u>	<u>0.13</u>			1.01	0.11
540C	0.76		<u>1.01</u>	<u>0.09</u>			1.01	0.09
585	<u>1.32</u>	<u>0.24</u>					1.32	0.24
586	<u>1.90</u>	<u>0.15</u>					1.90	0.15
589	<u>1.34</u>	<u>0.11</u>					1.34	0.11
592	<u>1.30</u>	<u>0.23</u>					1.30	0.23
595	<u>1.87</u>	<u>0.15</u>					1.87	0.15
596	<u>0.96</u>	<u>0.04</u>					0.96	0.04
599	<u>1.76</u>	<u>0.12</u>					1.76	0.12
601			<u>0.47</u>	<u>0.06</u>			1.02	0.06
602	<u>0.87</u>		0.31	0.20			0.87	
338	<u>1.22</u>		0.64	0.21	0.92		1.22	
339	<u>1.22</u>	<u>0.11</u>	0.86		-0.12		1.22	0.11
347	<u>1.16</u>	<u>0.07</u>	0.82	0.06	-0.16		1.16	0.07
394			1.52	0.01	<u>0.98</u>		1.28	
395			1.54		<u>0.80</u>	<u>0.02</u>	1.1	0.02
396	<u>1.22</u>	<u>0.22</u>	1.76		0.92		1.22	0.22
Canyon \emptyset			0.52	0.04			0.80	0.07
Slope \emptyset			0.39	0.09			1.00	0.06

877



878 Table 2 (continued)

Site	$\delta^{13}\text{C}_{U_{med}}$ stained (‰ VPDB)	st. dev. (‰)	$\delta^{13}\text{C}_{U_{med}}$ unstained (‰ VPDB)	st. dev. (‰)	$\delta^{13}\text{C}_{U_{med}}$ stained (>600 μm) (‰ VPDB)	st. dev. (‰)	$\delta^{13}\text{C}_{U_{med}}$ unstained (>600 μm) (‰ VPDB)	st. dev. (‰)	$\Delta\delta^{13}\text{C}_{U_{med-Epi}}$ stained (>600 μm) (‰)	st. dev. (‰)	$\Delta\delta^{13}\text{C}_{U_{med-Epi}}$ unstained (>600 μm) (‰)	st. dev. (‰)
537	0.17	0.38	-0.88	0.16	0.35	0.26	-0.82	0.03	-0.76	0.58	-1.93	0.35
540A	-0.46	0.21			-0.21	0.09			-1.29	0.30		
540B	0.13	0.32	0.19	0.35	0.27	0.23	0.46	0.10	-0.74	0.34	-0.55	0.21
540C	-0.14	0.30	0.06	0.32	0.05	0.26	0.28	0.32	-0.97	0.41	-0.74	0.47
585	0.58	0.22	0.50	0.47	0.58	0.22	0.50	0.22	-0.74	0.46	-0.82	0.46
586			0.95	0.46			1.11	0.31			-0.79	0.46
589			0.51	0.46			0.73	0.39			-0.61	0.50
592	-0.14	0.02	0.15	0.25	-0.12	0.00	0.24	0.20	-1.42	0.23	-1.06	0.43
595	0.09	0.53	0.67	0.41	0.37	0.31	0.77	0.41	-1.49	0.46	-1.09	0.56
596	-0.38	0.38	-0.43	0.34	-0.23	0.33	-0.27	0.27	-1.19	0.37	-1.23	0.31
599	0.03	0.26	0.25	0.45	0.12	0.20	0.41	0.28	-1.63	0.32	-1.35	0.40
601	-0.53	0.27	-0.47	0.38	-0.34	0.14	-0.37	0.35	-1.36	0.20	-1.39	0.41
602	-1.11	0.31	-1.09	0.27	-0.98	0.32	-1.13	0.26	-1.85	0.32	-2.00	0.26
338	-0.05	0.26	0.29	0.37	0.07	0.28	0.55	0.23	-1.15	0.28	-0.67	0.23
339	0.02	0.46	0.06	0.20	0.22	0.28	0.16	0.19	-0.99	0.39	-1.06	0.30
347	-0.19	0.25	0.02	0.17	-0.13	0.13	0.41	0.00	-1.29	0.20	-0.75	0.07
394	0.58	0.31	0.61	0.23	0.64	0.26	0.71	0.13	-0.64	0.27	-0.58	0.14
395	0.47	0.30	0.53	0.21	0.53	0.27	0.63	0.13	-0.57	0.27	-0.46	0.13
396	0.66	0.22	-0.64	0.60	0.72	0.19	-0.91	0.42	-0.50	0.29	-2.13	0.52
Canyon \emptyset	-0.32	0.29	-0.32	0.27	-0.17	0.20	-0.21	0.26	-0.97	0.27	-1.01	0.33
Slope \emptyset	0.26	0.30			0.33	0.26			-0.67	0.32		

879



880 Table 3.

<i>U. mediterranea</i> stained				
site	n	linear fit	R-squared	p-value
537	24	$Y = 0.001379 * X - 1.810017$	0.67	$1.1065 * e^{-6}$
540A	23	$Y = 0.001007 * X - 1.770373$	0.70	$5.746 * e^{-7}$
540B	14	$Y = 0.001257 * X - 1.7208851$	0.54	0.0027
540C	46	$Y = 0.000943 * X - 1.639236$	0.55	$3.769 * e^{-6}$
585	3	$Y = -0.00224 * X + 1.222667$	1.00	0.0082
592	2	$Y = 0.00034 * X - 1.6535$	1.00	X
595	10	$Y = 0.002013 * X - 3.012139$	0.75	0.0012
596	7	$Y = 0.001822 * X - 2.490764$	0.60	0.0401
599	10	$Y = 0.001600 * X - 2.789560$	0.49	0.0289
601	11	$Y = 0.001322 * X - 2.497314$	0.70	0.0013
602	15	$Y = 0.001143 * X - 2.709099$	0.41	0.0102
338	10	$Y = 0.001498 * X - 2.265059$	0.72	0.0020
339	12	$Y = 0.001527 * X - 2.323114$	0.48	0.0124
347	7	$Y = 0.001126 * X - 2.119201$	0.68	0.0232
394	19	$Y = 0.000968 * X - 1.680654$	0.27	0.0221
395	23	$Y = 0.001509 * X - 2.135640$	0.40	0.0012
396	20	$Y = 0.000789 * X - 1.304866$	0.39	0.0034
Canyon aug	7	$Y = 0.000516 * X - 1.297794$	0.45	0.1015
Canyon feb	21	$Y = 0.000701 * X - 1.634263$	0.43	0.0012
Slope aug	6	$Y = 0.000671 * X - 1.207976$	0.34	0.2244
Slope feb	14	$Y = 0.001223 * X - 1.518849$	0.48	0.0060
<i>U. mediterranea</i> unstained				
site	n	linear fit	R-squared	p-value
537	7	$Y = 0.000408 * X - 2.169793$	0.33	0.1784
540B	16	$Y = 0.001017 * X - 1.457536$	0.80	$2.4803 * e^{-6}$
540C	9	$Y = 0.000938 * X - 1.343878$	0.53	0.0270
585	4	$Y = 0.001610 * X - 1.910093$	0.85	0.0808
586	29	$Y = 0.001555 * X - 2.035859$	0.48	$2.9156 * e^{-5}$
589	25	$Y = 0.001612 * X - 1.917381$	0.58	$1.0482 * e^{-5}$
592	28	$Y = 0.001001 * X - 1.826222$	0.48	$4.5201 * e^{-5}$
595	36	$Y = 0.000841 * X - 1.740275$	0.17	0.0130
596	37	$Y = 0.001065 * X - 2.004262$	0.30	0.0005
599	12	$Y = 0.001031 * X - 2.201211$	0.31	0.0600
601	21	$Y = 0.000312 * X - 1.871316$	0.04	0.3927
602	14	$Y = -0.000427 * X - 1.697763$	0.12	0.2159
338	10	$Y = 0.001343 * X - 1.735480$	0.90	$3.0586 * e^{-5}$
339	9	$Y = 0.000456 * X - 1.408000$	0.31	0.1197
347	10	$Y = 0.000615 * X - 1.400530$	0.71	0.0023
394	22	$Y = 0.000573 * X - 1.221329$	0.32	0.0060
395	15	$Y = 0.000544 * X - 1.301955$	0.33	0.0256
396	17	$Y = -0.001682 * X - 1.020989$	0.50	0.0016
Canyon aug	36	$Y = 0.000584 * X - 1.469912$	0.28	0.0009



881 **Figure captions**

882

883 Figure 1. Location of the study areas in the Mediterranean Sea and regional bathymetric maps
884 with locations of sample sites in the (a) Mallorca Channel, (b) Alboran Sea, (c) Gulf of Lions
885 and Spanish Slope off Barcelona, (d) Strait of Sicily, and (e) Aegean Sea.

886

887 Figure 2. (a) The $\delta^{13}\text{C}$ signals of epifaunal species (*Cibicidoides pachydermus*, *Cibicides*
888 *lobatulus*, *Planulina ariminensis*) with estimated $\delta^{13}\text{C}_{\text{Epi}}$ value for each investigated site.
889 Symbol sizes indicate different test sizes. Red symbols mark relocated fossil tests. Green
890 circles show $\delta^{13}\text{C}_{\text{DIC}}$ value of the bottom water approximated after $\delta^{13}\text{C}_{\text{Epi}}$ values. (b) The
891 $\delta^{13}\text{C}_{\text{Epi}}$ versus water depth shows a wider scattering for the Aegean Sea, than for the Western
892 Mediterranean.

893

894 Figure 3. Ontogenetic trends in the $\delta^{13}\text{C}$ difference between *Uvigerina mediterranea* and
895 epifaunal taxa ($\Delta\delta^{13}\text{C}_{\text{Umed-Epi}}$) based on different size classes of *U. mediterranea*. Data shown
896 are for live (rose Bengal stained) and dead (unstained) individuals of *U. mediterranea* and for
897 the western Mediterranean Sea (left) and Aegean Sea (right). Dashed lines represent already
898 published data (Schmiedl et al., 2004; Theodor et al., 2016).

899

900 Figure 4. The $\delta^{13}\text{C}$ difference between live *Uvigerina mediterranea* and epifaunal taxa
901 ($\Delta\delta^{13}\text{C}_{\text{Umed-Epi}}$) plotted against (a) Median Living Depth (MLD), (b) depth of redox boundary, (c)
902 total organic carbon (TOC) content, (d, e) Primary Production in surface waters of the year
903 previous to sampling. The satellite derived PP was calculated with the algorithms of Antoine &
904 Morel, 1996 (d) and Uitz et al., 2008 (e).

905

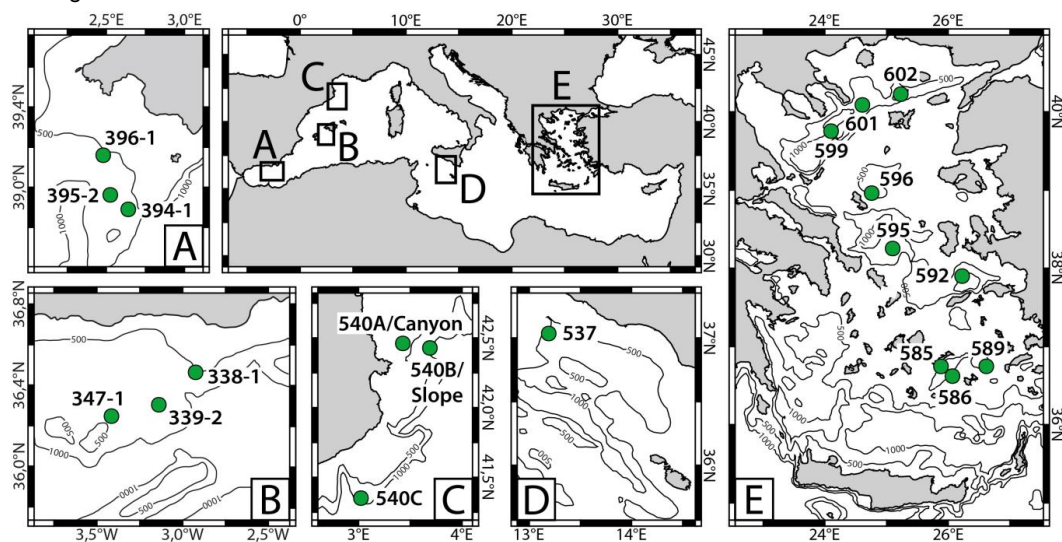
906 Figure 5. The $\delta^{13}\text{C}$ difference between live and dead *Uvigerina mediterranea* and epifaunal
907 taxa ($\Delta\delta^{13}\text{C}_{\text{Umed-Epi}}$) against organic carbon flux rates (C_{org} flux) calculated from primary



908 productivity in surface waters after Betzer et al. (1984). As in figure 4, satellite derived Primary
909 Production values of Antoine & Morel (1996) (top) and Uitz et al., (2008) (bottom) were used.
910
911 Figure 6: Correlation of the $\delta^{13}\text{C}$ difference between live *Uvigerina mediterranea* and epifaunal
912 taxa ($\Delta\delta^{13}\text{C}_{Umed-Epi}$) and organic carbon flux rate (C_{org} flux) calculated according to Antoine &
913 Morel (1996) and Betzer et al. (1984). Transparent data from the central and northern Aegean
914 Sea and the Gulf of Lions have been removed from the function since PP-based C_{org} flux values
915 are likely underestimated because of the additional influence of lateral organic matter fluxes
916 on the $\delta^{13}\text{C}_{Umed}$ values in these areas.



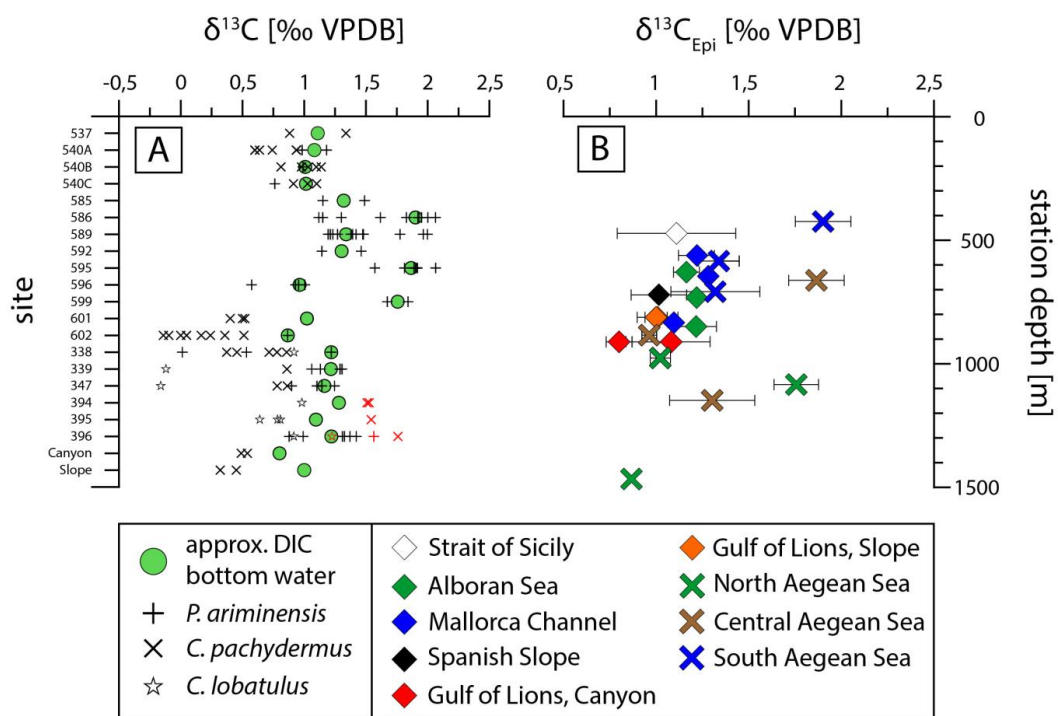
917 Figure 1



918



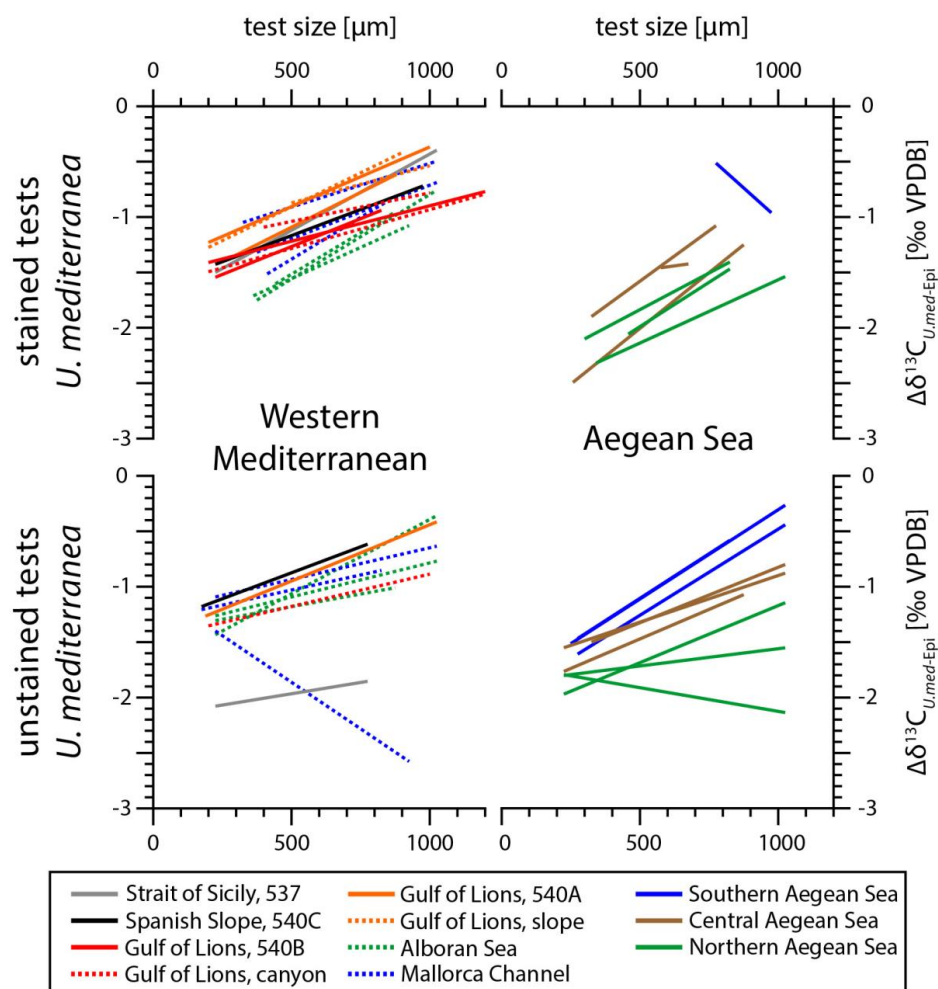
919 Figure 2.



920



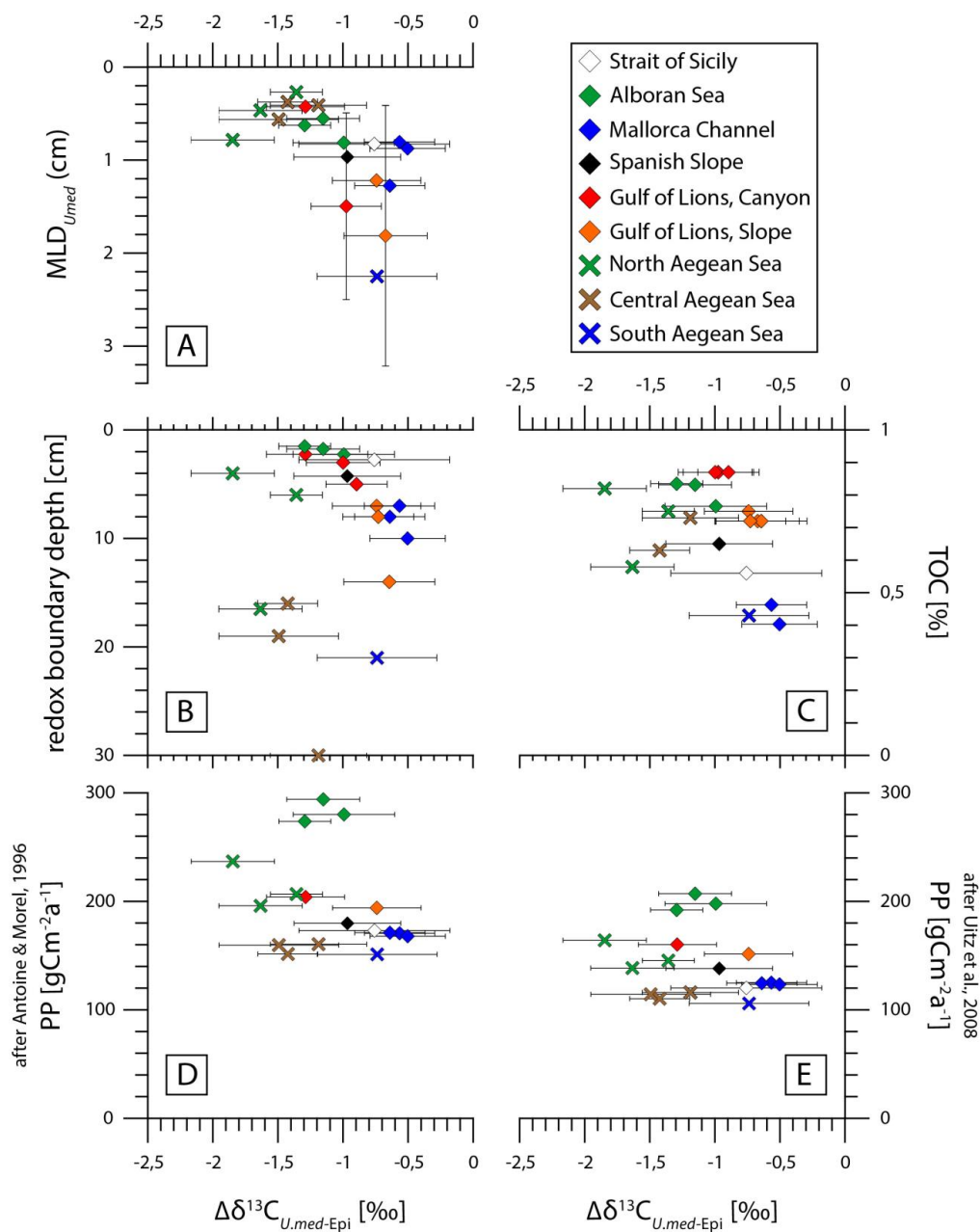
921 Figure 3.



922



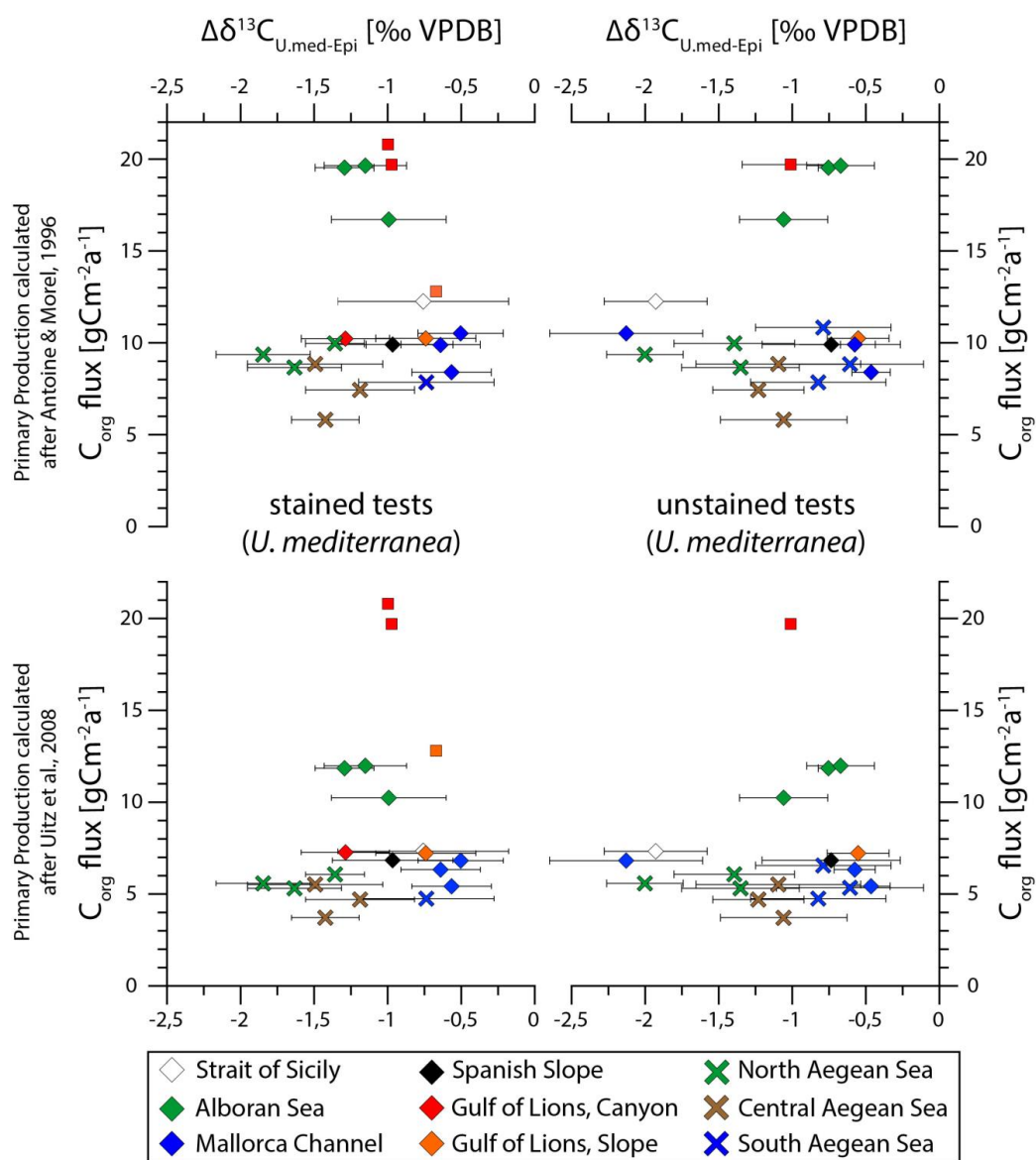
923 Figure 4.



924



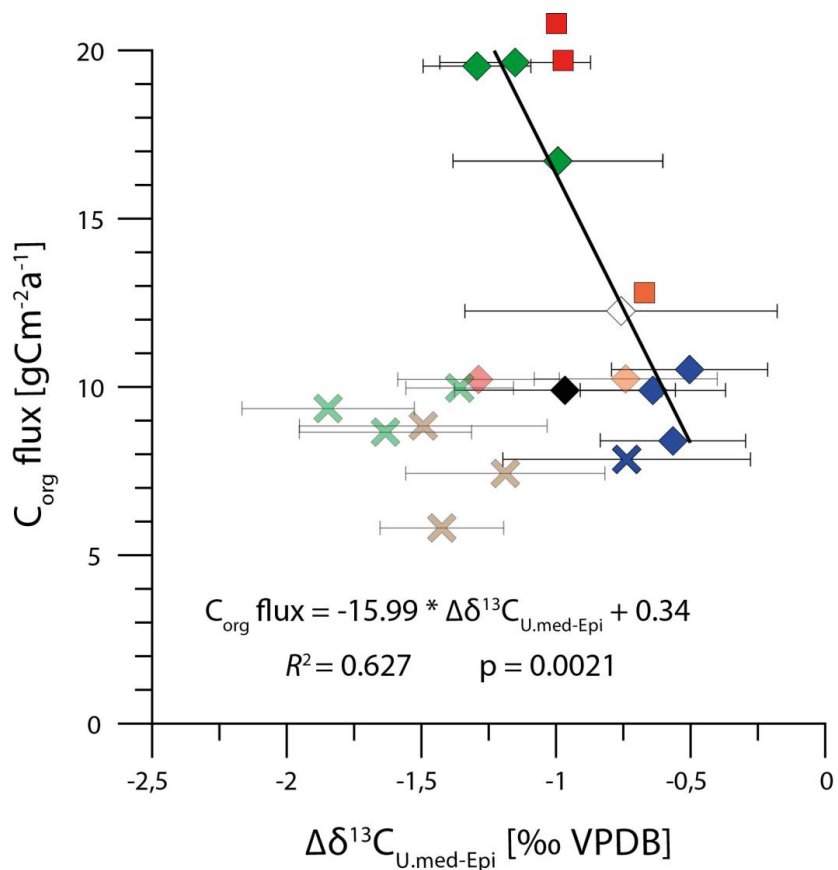
925 Figure 5.



926



927 Figure 6.



◇ Strait of Sicily	◆ Spanish Slope	✕ North Aegean Sea
◆ Alboran Sea	◆ Gulf of Lions, Canyon	✕ Central Aegean Sea
◆ Mallorca Channel	◆ Gulf of Lions, Slope	✕ South Aegean Sea